

UNIVERSITÀ DELLA CALABRIA



Dipartimento di Farmacia e Scienze della Salute e della Nutrizione

---

**Dottorato in Medicina Traslazionale  
XXIX Ciclo**

*Settore Scientifico: MED/05*

**Activated FXR Inhibits Leptin Signaling and  
Counteracts Tumor-promoting Activities of  
Cancer-Associated Fibroblasts in Breast *Malignancy***

*Dottoranda:*  
**Valentina VIRCILLO**

*Coordinatore Dottorato:*  
Ch.mo Prof.  
**Sebastiano ANDÒ**

*Tutor Dottorando:*  
Ch.ma Prof.ssa  
**Stefania CATALANO**

---

*Anno Accademico 2015-2016*

*A te che mi hai sostenuta  
solo grazie a te, oggi, tutto questo si è realizzato!  
Grazie a noi due e alla forza che tu, ogni giorno,  
con il tuo amore mi hai donato!*

*A mio marito, mio unico amore.*

*Alla mia famiglia, con infinito amore!*

*Ai miei splendidi nonni!*

*Alla mia dolce Maggie!*

# Abstract

Cancer-associated fibroblasts (CAFs), the principal components of the tumor stroma, play a central role in cancer development and progression. As an important regulator of the crosstalk between breast cancer cells and CAFs, the cytokine leptin has been associated to breast carcinogenesis. The nuclear Farnesoid X Receptor-(FXR) seems to exert an oncosuppressive role in different tumors, including breast cancer. In this study, we demonstrated, for the first time, that the synthetic FXR agonist GW4064, inhibiting leptin signaling, affects the tumor-promoting activities of CAFs in breast malignancy. GW4064 inhibited growth, motility and invasiveness induced by leptin as well as by CAF-conditioned media in different breast cancer cell lines. These effects rely on the ability of activated FXR to increase the expression of the suppressor of the cytokine signaling 3 (SOCS3) leading to inhibition of leptin-activated signaling and downregulation of leptin-target genes. We further extend our data investigating whether FXR agonist may directly influence CAF phenotype. We demonstrated that FXR is expressed in different CAFs and treatment with GW 4064 is able to induce the transcription of key FXR target genes, including SHP (Small Heterodimer Partner) and BSEP (Bile Salt Export Pump). Interestingly, FXR activation is able to significantly reduce CAF motility, without influencing their proliferation capabilities. Accordingly, IPA (Ingenuity Pathway Analysis) on FXR-modulated genes highlighted cellular movement as the most significantly

represented biologic process and evidenced a marked reduction in the activity of Rho signaling and Integrin proteins, with activation z-score of -1, -0,5 respectively. Moreover, our data showed a reduction in stress fibers formation in GW 4064-treated CAFs. Activated FXR is able to reduce tumor promoting effects of CAFs on breast cancer cells, due to the ability of GW 4064 to reduce CAF secreted soluble factors, including IGF-1 (Insulin Growth Factor-1), FGF-9 (Fibroblast Growth Factor 9), TGF- $\beta$ 3 (Transforming Growth Factor Beta 3) and others key mediators involved in the crosstalk tumor-stroma. Indeed, our data demonstrate how ER- $\alpha$  breast cancer cell lines, MCF-7 and T47D, cocultured with conditioned media derived from GW4064-treated CAFs, exhibit a significantly reduced anchorage-independent growth and migration. In vivo xenograft studies, using MCF-7 cells alone or co-injected with CAFs, showed that GW4064 administration markedly reduced tumor growth. Thus, FXR ligands might represent an emerging potential anti-cancer therapy able to block the tumor supportive role of activated fibroblasts within the breast microenvironment.

# Table of Contents

<b>Introduction</b>	Pag.	6
<b>Materials and Methods</b>	»	18
Reagents and antibodies	»	18
Cell Culture	»	20
Cancer Associate Fibroblasts (CAFs) isolation	»	20
Conditioned medium (CM) derived from CAFs	»	21
Leptin measurement by ELISA	»	21
Immunofluorescence	»	22
Soft Agar assays	»	22
Wound Healing assays	»	22
Invasion assays	»	23
Transmigration assays	»	23
Reverse transcription and real-time reverse transcriptase PCR assays	»	24
RNA library preparation and sequencing	»	27
Phalloidin staining	»	28
Immunoblot analysis	»	28
Transient transfection assays	»	29
<i>In vivo</i> experiments	»	29
Histopathological analysis	»	31
Immunohistochemical analysis	»	31
Statistical analyses	»	32
<b>Results</b>	»	33
Activated FXR Inhibits Leptin-Induced Growth and Motility in Breast Cancer Cells	»	34
GW4064 Reduces Leptin Signaling Pathway Activation and Leptin Target Gene Expression in Breast Cancer Cells	»	36
GW4064 Reverses CAF-Induced Breast Cancer Cell Growth and Motility	»	42
Impact of FXR activation in SKBR3 breast cancer cells	»	46
The FXR ligand GW4064 Inhibits Tumor Growth in MCF-7/CAF xenografts	»	48

FXR Expression and Activation in CAFs	» 52
Impact of Activated FXR on Motility and Proliferation in CAFs	» 55
GW 4064-treated CAFs Exhibit a Reduction in the Activity of Rho-GTPase and Integrin Signaling	» 56
GW 4064 Treatment Reduced Secretion of CAFs Soluble Factors	» 61
Breast Cancer Cells Cocultured with GW 4064-treated CAFs Showed Reduced Anchorage-Independent Growth and Motility	» 63
<b>Discussion</b>	» 65
<b>References</b>	» 74

---

# INTRODUCTION

---

Despite major advances in understanding the molecular basis of tumor, breast cancer remains the major leading cause of cancer-related death in women worldwide (*Jemal A. et al., 2010*). In 2014, the average incidence of occurrence of breast cancer for a woman has been calculated to be 1 in 8 (*Cancer Research UK, <http://www.cancerresearchuk.org/>*), but it severely increases if one or more of the many well-known risk factors coexist. An increasing number of studies are revealing how among all predisposing factors, obesity has the main impact on breast development and prognosis in postmenopausal woman. Indeed, prospective epidemiological studies have shown that excessive adiposity strongly influences risk, prognosis and progression of breast cancer (*Calle EE. et al., 2004; Renehan AG. et al., 2008*). Female breast cancer patients who are obese at the time of the diagnosis are more likely to have a worse prognosis and a higher risk of recurrence regardless of therapy than lean patients (*Protani M. et al., 2010; Renehan AG et al., 2010*). A meta-analysis of 43 studies, that enrolled women diagnosed with breast cancer over a long period (1963-2005) also estimated a 33% increase in the rate of death among obese women (*Protani M. et al., 2010*). Several hypotheses have been proposed to unravel the direct link

between obesity and breast cancer and these include hyperinsulinemia, estrogen signaling, inflammation and adipokine expression (*Taubes G. et al., 2012; Park J. et al., 2011*). Undoubtedly, the revised concept of adipose tissues from an inert depot for body energy to endocrine and immunologically active organs placed particular emphasis on the potential role of adipokines in various biological processes. Acting through endocrine, paracrine and autocrine mechanisms, adipokines, that are not only produced by adipocytes but also by stromal cells (mainly fibroblasts), macrophages and cancer cells, impact the development and progression of obesity-related cancers (*Park J. et al., 2011*). Among adipokines, leptin, whose circulating levels increase in proportion to fat mass, has been recognized as a crucial mediator of molecular effects of obesity on breast cancer (*Ando S. et al., 2014; Ando S. et al., 2012*). Leptin, a 16 kDa peptide resulting as a product of the obese (*Ob*) gene, is a pleiotropic molecule that influences appetite control, energy balance, immune response, reproduction, haematopoiesis, bone development, angiogenesis and proliferation of different cell types including cells of the breast (*Ando S. et al., 2014; Ando S. et al., 2012*). Biological activities of leptin are mediated through

binding to the transmembrane receptor (Ob-R), a member of the class I cytokine receptor superfamily, that includes six isoforms different in the length of their intracellular tails. Leptin binding to the extracellular domain of the long isoform of leptin receptor leads to the activation of a broad array of multiple intracellular downstream signaling pathways, including Janus kinase 2-signal transducer and activator of transcription 3 (JAK2/STAT3), mitogen-activated protein kinase (MAPK), and phosphatidylinositol 3-kinase-protein kinase B (PI3K/Akt) pathways (Cirillo D. et al., 2008) (Figure 1).

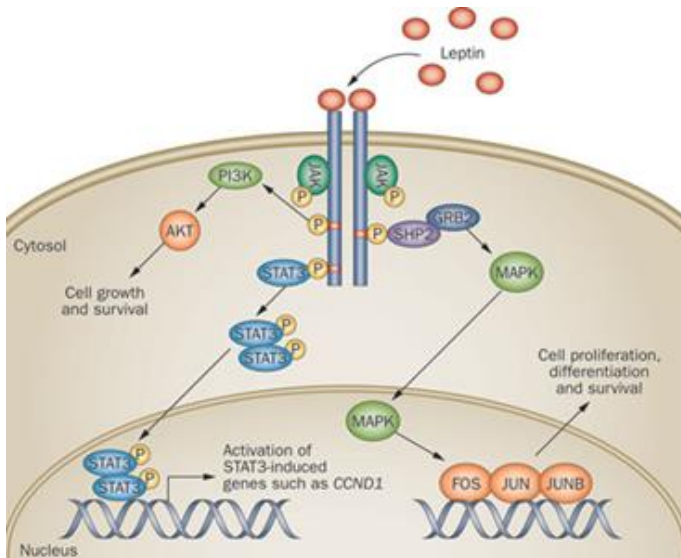


**Figure 1: Leptin Signaling.** Binding of Leptin to its receptor, Ob-R, results in the activation of its downstream pathways such as JAK2-STAT3, mitogen-activated protein kinase (MAPK), and phosphatidylinositol 3-kinase/protein kinase B (PI3K/AKT).

A plethora of clinical and experimental studies strongly support the idea that leptin activity is correlated with breast cancer occurrence and tumor behavior. Interestingly, leptin and both isoform of leptin receptor are overexpressed in breast cancer biopsies compared with healthy epithelium and benign lesions (*Garofalo C. et al., 2006; Ishikawa M. et al., 2004; Miyoshi Y. et al., 2006; Revillion F. et al., 2006; Jarde T. et al., 2008*). Moreover, the expression of leptin and Ob-R were positively correlated, suggesting that leptin acts on mammary tumor cells via an autocrine pathway. Additionally, a strong correlation between tumor expression of leptin/leptin receptor and grade of the tumor, occurrence of metastasis and poor prognosis was observed (*Garofalo C. et al., 2006; Ishikawa M. et al., 2004; Miyoshi Y. et al., 2006; Jarde T. et al., 2008; Fiorio E. et al., 2008*). Kaplan-Meier survival analysis indicated that Ob-R expression was associated with reduced overall survival in breast carcinoma patients, especially in those with basal-like subtypes (*Giordano C. et al., 2016*). It has been extensively demonstrated using both *in vivo* and *in vitro* experimental models that the adipokine leptin modulates many aspects of breast cancer biology from initiation and primary tumor growth to

metastatic progression. In addition, crosstalk with other different signaling molecules, such as estrogens, growth factors, Notch and inflammatory cytokines, further increases leptin impact on breast tumor progression (Fiorio E. et al., 2008; Barone I. et al., 2012; Catalano S. et al., 2003; Catalano S. et al., 2004; Giordano C. et al., 2013; Saxena NK. et al., 2008; Guo S. et al., 2011) (Figure 2).

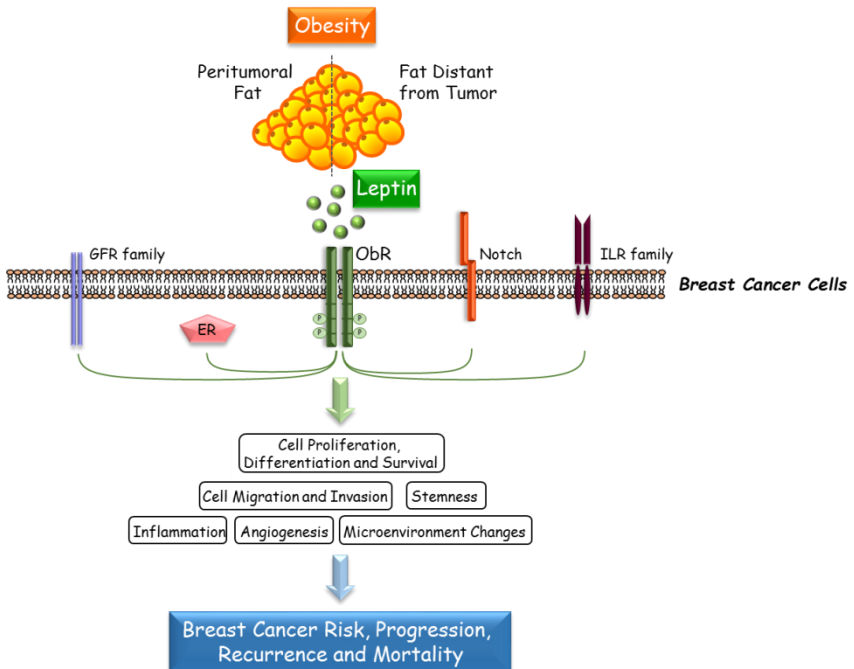


**Figure 2: Crosstalk Between Leptin and Other Different Signaling Molecules.**

Leptin interacts with multiple oncogenic pathways, including growth factor, estrogen, Notch and inflammatory cytokine signaling, to further affect various steps of breast tumor progression.

Interestingly, we previously demonstrated that leptin is also secreted by a subpopulation of fibroblasts, known as Cancer-associated Fibroblasts (CAFs), within the tumor microenvironment, and that CAFs-secreted leptin promotes proliferation, migration, and invasiveness of breast cancer cells (*Barone I. et al., 2012*). Since Paget's "Seed and Soil" hypothesis (*Paget S. et al., 1889*) on distribution of secondary growths in breast cancer, it took more than 100 years to definitively demonstrate that the phenotype of malignant cells is strictly dependent on heterotypic signals coming from stromal cells in the surrounding microenvironment. The tumor microenvironment contains a number of cell types, including mesenchymal stem cells (MSCs), CAFs, adipocytes, endothelial and immune cells, all of which, through networks of cytokines and growth factors, have been shown to influence tumor growth and metastasis (*Korkaya H. et al., 2011*) (Figure 3).

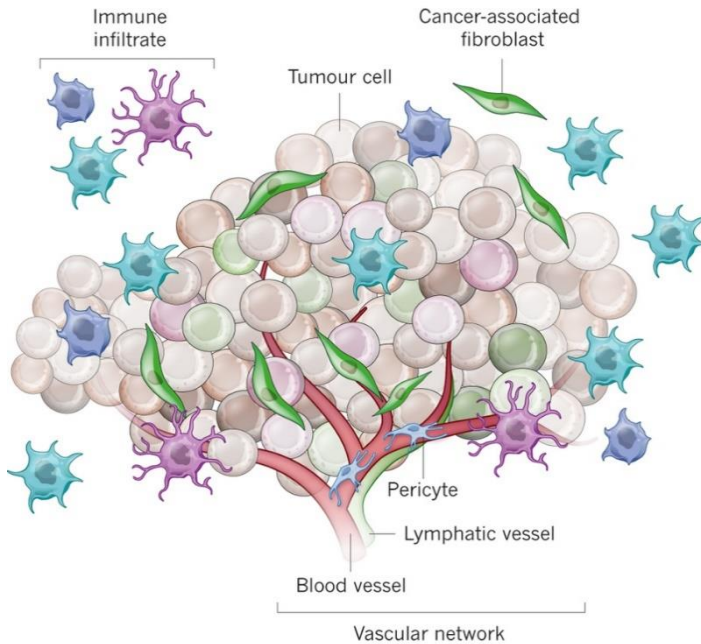


**Figure 3: Schematic Representation of Tumor Microenvironment.**

Indeed, stromal cells influence tumor invasiveness and malignancy, whereas at the onset and during breast cancer progression, the microenvironment is reorganized by cancer cells. In the almost all solid tumor microenvironment, CAFs are present in aberrantly high numbers and are distinct from normal fibroblasts, involved in the healthy tissue homeostasis (Aboussekhra A. et al., 2011). Particularly, in breast malignancies, CAFs exert a pivotal role in tumor onset and progression through multiple mechanisms, such as affecting

estradiol levels, secreting increasing levels of growth factors, chemokines, cytokines and matrix metalloproteinases (MMPs), inducing epigenetic changes, epithelial to mesenchymal transition (EMT) and stemness. More importantly, CAFs not only induce mammary carcinogenesis but also promote therapeutic resistance, which contributes to breast cancer progression and poor prognosis. Thus, targeting specific CAFs-secreted factors, such as leptin, may provide more effective treatment options to achieve therapeutic benefits in breast cancer patients.

The Farnesoid X receptor (FXR) is an adopted member of the metabolic nuclear receptor superfamily, mainly expressed in the liver and in the gastrointestinal tract, where it regulates expression of genes involved in bile acids, cholesterol and triglyceride metabolism (*Forman B.M. et al., 1995; Makishima M. et al., 1999; Parks D.J. et al., 1999*) (Figure 4).

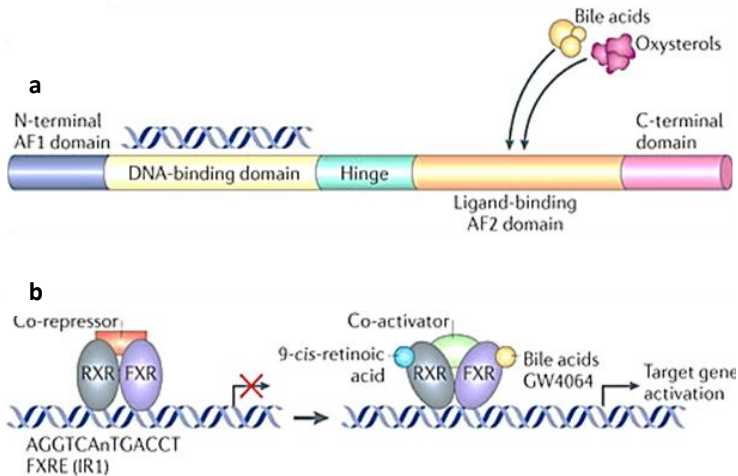


**Figure 4: FXR Structure and Mechanism of Action.**

(a) The basic structure of a nuclear receptor, highlighting the DNA-binding and ligand-binding domains. (b) Liver X receptor (LXR) forms an obligate heterodimer with retinoid X receptor (RXR) that binds to a DR4 (direct repeat spaced by four nucleotides) LXRE (LXR response element) in the regulatory regions of target genes, thereby repressing gene expression. Following ligand binding to LXR or RXR, the heterodimer changes conformation, which leads to the release of co-repressors and the recruitment of co-activators. This results in the transcription of target genes. Similarly, farnesoid X receptor (FXR) forms a heterodimer with RXR and binds to the FXR response element (FXRE), which is typically an inverse repeat spaced by one nucleotide (IR1), in its target genes to induce gene expression. AF domain, activation function domain; C-terminal, carboxy-terminal; N-terminal, amino-terminal.

Upon activation by its natural ligands, such as bile acids and their metabolites, or by synthetic agonists including GW4064, FXR regulates the expression of its target genes by binding either as a monomer or as a heterodimer with RXR $\alpha$  to genomic FXR responsive elements (FXREs) (Calkin and Tontonoz, 2012; Modica S. et al., 2010; Wang et al., 2008).

Recent findings extend its function in several nonenterohepatic tissues, including its control in regulating cell growth and carcinogenesis. Indeed, separate studies have established both positive and negative correlations between FXR expression and cancer (*Catalano S. et al. 2012; Catalano S. et al. 2010; Kim I. et al. 2007; Yang F. et al. 2007; Modica S. et al. 2008; Maran R.R. et al. 2009; Dai J. et al. 2011; Peng Z. et al. 2012*). Particularly, in breast cancer cell lines FXR agonists inhibit aromatase expression reducing local estrogens production and induce apoptosis (*Swales K.E. et al., 2006*), whereas other authors have reported that FXR activation stimulates breast cancer cell proliferation (*Journe F. et al., 2008*). Besides, we have shown that activated FXR decreases tamoxifen-resistant breast cancer cell growth reducing the membrane tyrosine kinase receptor HER2 expression and signaling (*Giordano C. et al., 2012*). It has also been demonstrated that FXR activation by natural and synthetic ligands represses the expression of inflammatory cytokines and chemokines (*Rizzo G. et al., 2006; Vavassori P. et al., 2009*). Thus, FXR can be considered more than a metabolic regulator, and FXR ligands may represent an important

research issue to provide an alternative therapeutic strategy for the treatment of breast cancer.

On the basis of the above observations, the aim of the current study was:

To evaluate, using both *in vitro* and *in vivo* experimental models, the role of Farnesoid X Receptor to negatively impact the cancer promoting activities of CAFs.

Particularly, we investigated:

- i) the ability of activated FXR in interfering with tumour microenvironment pressure exerted by CAFs, with a special focus on the signalling of the adipokine leptin;
- ii) the function of FXR in CAFs and whether this receptor may affect their phenotype.

---

# MATERIALS AND METHODS

---

**Reagents and antibodies.** GW4064 from Tocris Bioscience (Bristol, UK). Z-Guggulsterone from Santa Cruz. L-glutamine, penicillin, streptomycin, aprotinin, leupeptin, phenylmethylsulfonyl fluoride (PMSF), sodium orthovanadate, NP-40, MTT and anti- $\alpha$  SMA antibody were purchased from Sigma (Milan, Italy). Dulbecco's Modified Eagle's Medium (DMEM), DMEM-F12, RPMI, McCoy's5A, Hank's balanced salt solution, fetal bovine serum (FBS), Leptin, TRIzol, TaqDNA polymerase, RETROscript kit, 100-bp DNA ladder were from Life Technologies (Monza MB, Italy). Antibodies against FXR (sc-13063), Survivin (sc-17779), Cyclin D1 (sc-4074), Ob (sc-4912), KI67 (sc-15402), Cytokeratin 18 (sc-32329), and  $\beta$  - Actin (sc-47778), by Santa Cruz Biotechnology (Santa Cruz, CA, USA); anti-SOCS3 (ab-16030) antibody by Abcam (Cambridge, UK). Antibodies against Rho (#2117), Rac (#2465), CDC42 (#2466), total non-phosphorylated (#3230) and Phosphorylated (p) JAK2 (Tyr1007/1008) (#8082), STAT3 (Tyr705) (#9131), Akt (Ser473) (#9271), and MAPK (Thr202/Tyr204) (#9101) were purchased from Cell Signaling Technology (Beverly, MA, USA).

**Cell culture.** MCF-7, MDA-MB-231, T47D and SKBR3 human breast cancer cell lines were acquired from American Type Culture Collection (Manassas, VA, USA) where they were authenticated, stored according to supplier's instructions, and used within 4–6 months after frozen aliquots resuscitations. MCF-7 cells were cultured in DMEM medium containing 10% FBS, 1% L-glutamine, 1% Eagle's nonessential amino acids, and 1 mg/ml penicillin-streptomycin at 37 °C with 5% CO<sub>2</sub> air. MDA-MB-231 cells were grown in DMEM: F12 containing 10% FBS. T47D cells in RPMI medium with 10% FBS and 0,2 U/ml insulin. SKBR3 cells were cultured in McCoy's5A Medium modified containing 10% FBS. All cell lines were used within six-months after frozen aliquot resuscitations and regularly tested for Mycoplasma-negativity (MycoAlert, Lonza). Before each experiment, cells were grown in phenol red-free medium, containing 5% charcoal-stripped FBS (cs-FBS) for 2 days and treated as described.

**CAF isolation.** Human breast cancer specimens were collected in 2013–2014 from four primary tumors of patients who signed informed consent in accordance with approved Human Subject's guidelines at Annunziata Hospital (Cosenza, Italy). Following tumor excision, small pieces were digested (500 IU

collagenase in Hank's balanced salt solution; Sigma; 37 °C for 2 h). After differential centrifugation ( $90 \times g$  for 2 min), the supernatant containing CAFs was centrifuged ( $500 \times g$  for 8 min), resuspended, and cultured in RPMI-1640 medium supplemented with 15% FBS and antibiotics. CAFs between 4 and 10 passages were used, tested by mycoplasma presence (MycoAlert Mycoplasma Detection Assay, Lonza), and authenticated by  $\alpha$  SMA and fibroblast activation protein (FAP) expression. Study was approved by ethics institutional committees at Annunziata Hospital. Experimental procedures for CAF isolation were carried out in accordance with the approved guidelines.

**Conditioned medium (CM) derived from CAFs.** CAFs were treated with vehicle (-) or with GW4064 (GW,  $6\mu\text{M}$ ) in presence or not of Z-Guggulsterone (Gugg,  $20\mu\text{M}$ ). After 24 hrs, conditioned media was collected. After collection, conditioned media was centrifuged to remove cellular debris, and used in respective co-culture experiments.

**Leptin measurement by ELISA.** Leptin was measured by ELISA (LDN, Nordhorn, Germany) following manufacturer's protocol. Results are presented as nanograms per mg of protein.

**Immunofluorescence.** Cells were fixed with 4% paraformaldehyde, permeabilized with PBS 0.2% Triton X-100 followed by blocking with 5% bovine serum albumin (1 hour at room temperature), and incubated with anti- $\alpha$ -SMA (Sigma) and anti-FXR (Santa Cruz) (4C, overnight) and with fluorescein isothiocyanate–conjugated secondary antibody (30 minutes at room temperature). IgG primary antibody was used as negative control. 40, 6-Diamidino-2-phenylindole (DAPI; Sigma) staining was used for nuclei detection. Fluorescence was photographed with OLYMPUS BX51 microscope, 20X objective.

**Soft agar growth assays.** Cells (25,000 per well) were plated in 4 ml of 0.35% agarose with 5% CS-FBS in phenol red-free media, in a 0.7% agarose base in six-well plates. Two days after plating, media containing control vehicle or treatments was added to the top layer, and the media were replaced every two days. After 14 days, 150  $\mu$ l of MTT was added to each well and allowed to incubate at 37 °C for 4 h. Plates were then placed in 4 °C overnight and colonies >50  $\mu$ m diameter from triplicate assays were counted.

**Wound-healing assays.** Cell monolayers were scraped and treated as indicated. Wound closure was monitored over 12–

24 h; cells were fixed and stained with Coomassie brilliant blue. Pictures were taken at 10X magnification using phase-contrast microscopy and are representative of three independent experiments. The rate of wound healing was quantified from the images using Scion Image Program and Adobe Photoshop Program and standard deviations along with associated P values for the biological replicates were determined by using GraphPad-Prism4 software (GraphPad Inc., San Diego, CA).

**Invasion assays.** Matrigel-based invasion assay was conducted in invasion chambers (8- $\mu$  m membranes) coated with Matrigel (BD Biosciences; 0.4  $\mu$  g/mL). Cells treated with leptin, CAF-CM with or without GW4064 were seeded into top Transwell chambers, whereas regular full medium was used as chemoattractant in lower chambers. After 24 h (MDA-MB-231) and 36 h (MCF-7), invaded cells were fixed with 4% paraformaldehyde and stained with DAPI. Images represent 1 of 3 independent experiments (10X magnification).

**Transmigration assays.** CAFs and breast cancer cell lines treated with or without leptin, were placed in the upper compartments of Boyden chamber (8- $\mu$ m membranes/Corning Costar. Bottom well contained regular full media.

After 24 hours, migrated cells were fixed and stained with Coomassie brilliant blue. Migration was quantified by viewing 5 separate fields per membrane at 20 magnification and expressed as the mean number of migrated cells. Data represent 3 independent experiments, assayed in triplicate.

**Reverse transcription and real-time reverse transcriptase PCR assays.** Total RNA was extracted from cells using RNeasy columns (Qiagen) and the FXR, SOCS3, Ob, ObR, FAP, 36B4 gene expression was performed by the reverse transcription-PCR method using a RETROscript kit (Applied Biosystem). Gene expression profile of the other genes used in this study was performed by Real-time reverse transcription–PCR. Total RNA (2µg) was reverse transcribed with the RETROscript kit; cDNA was diluted 1:2 in nuclease-free water and 5µl were analysed in triplicates by real-time PCR in an iCycler iQ Detection System (Bio-Rad, USA) using SYBR Green Universal PCR Master Mix with 0.1 mmol/l of each primer in a total volume of 30 µl reaction mixture following the manufacturer’s recommendations. Negative control contained water instead of first strand cDNA was used. Each sample was normalized on its GAPDH mRNA content. The relative gene expression levels were normalized to a calibrator that was chosen to be the

basal, untreated sample. Final results were expressed as n-fold differences in gene expression relative to GAPDH mRNA and calibrator, calculated using the  $\Delta\text{Ct}$  method as follows:  $n\text{-fold} = 2^{-(\Delta\text{Ct}_{\text{sample}} - \Delta\text{Ct}_{\text{calibrator}})}$  where  $\Delta\text{Ct}$  values of the sample and calibrator were determined by subtracting the average Ct value of the GAPDH mRNA reference gene from the average Ct value of the gene analysed.

Primers used for the amplification were reported in Table 1.

**Table 1.** Primers sequences used for qRT-PCR

<i>Gene Symbol</i>	<i>Gene Name</i>	<i>Primer Sequences</i>
Ob	Leptin	For 5'-GAGACCTCCTCCATGTGCTG-3' Rev 5'-TGAGCTCAGATATCGGGCTGAAC-3'
FAP	Fibroblast activation protein	For 5'-AGAAAGCAGAAGCTGGATGG-3' Rev 5'-ACACACTTCTTGCTTGGAGGAT-3'
36B4	36B4	For 5'-CTCAACATCTCCCCCTTCTC-3' Rev 5'-CAAATCCCATATCCTCGT-3'
GAPDH	glyceraldehyde-3-phosphate dehydrogenase	For 5'-CCCACTCCTCCACCTTTGAC-3' Rev 5'-TGTTGCTGTAGCCAAATTCGT-3'
ObRL	Leptin Receptor Long Isoform	For 5'-GATAGAGGCCAGGCATTTTTTA-3' Rev 5'-CACCCTCTCTCTCTTTTGATTGA-3'
ObRS	Leptin Receptor Short Isoform	For 5'-ATTGTGCCAGTAATTATTTCTCTTCC-3' Rev 5'-CCACCATATGTAACTCTCAGAAGTTCA-3'
hFXR	Farnesoid X-Activated Receptor	For 5'-TACATGCGAAGAAAGTGTCAAGA-3' Rev 5'-ATCAGACCGTGAATGAAGACAGT-3'
CCL2	C-C Motif Chemokine Ligand 2	For 5'-CCCCAGTCACCTGCCTTAT-3' Rev 5'-GCTTCTTTGGGACACTTGCT-3'
CTGF	Connective tissue Growth Factor	For 5'-GCACAAGGGCCTATTCTGTC-3' Rev 5'-ACGTGCACTGGTACTTGCGAG-3'
HGF	Hepatocyte Growth Factor	For 5'-TGTGGGTGACCAACTCCTG-3' Rev 5'-TTTCCTTTGTCCCTCTGCAT-3'
PDGFD	Platelet Derived Growth Factor D	For 5'-ACTCTGATGCGGATGCTCT-3' Rev 5'-CGAGGGGTGTCAGATACAT-3'
FGF9	Fibroblast Growth Factor 9	For 5'-GAAAGACCACAGCCGATTTG-3' Rev 5'-TTCATCCCAGGTAGAGTCC-3'
TGF- $\beta$ 3	Transforming Growth Factor Beta 3	For 5'-GGTTTTCCGCTTCAATGTGT-3' Rev 5'-GCTCGATCCTCTGCTCATTC-3'
SHP	Small Heterodimer Partner	For 5'-CACTGGGTGCTGTGTGAAGT-3' Rev 5'-CCAATGATAGGGCGAAAGAA-3'
BSEP/ ABCB11	ATP binding cassette subfamily B member 11	For 5'-GGATCGAATCAAGGGTGAAA-3' Rev 5'-CTCCACTGGGTCTACCAGA-3'

**RNA library preparation and sequencing.** Total RNA was extracted from experimental models, according to supplier's instructions. RNA concentration was determined with NanoDrop-1000 spectrophotometer and quality assessed with Agilent-2100-Bioanalyzer and Agilent-RNA-6000 nanocartridges (Agilent Technologies). High quality RNA from three-independent purifications for each experimental point was used for library preparation. Indexed libraries were prepared from 1µg/ea. of purified RNA with TruSeq-RNASample- Prep-Kit (Illumina) following suppliers. Libraries quality controls were performed using Agilent-2100-Bioanalyzer and Agilent DNA-1000 cartridges and concentrations were determined with Qubit-2.0 Fluorometer (Life Technologies). Libraries were sequenced (paired-end, 2×100 cycles) at a concentration of 8pmol/L per lane on HiSeq2500 platform (Illumina) as described (Dago D.N. et al., 2015).

**Phalloidin staining.** Polymerized actin stress fibers were stained with Alexa Fluor 568-conjugated phalloidin, following manufacturers (Life Technologies). Cell nuclei were counterstained with DAPI. OLYMPUS-BX51 microscope (100X magnification) was used for imaging.

**Immunoblot analysis.** CAFs, MCF-7, MDA-MB-231, and SKBR3 cells were grown to 50–60% confluence and treated as indicated before lysis in 500  $\mu$  l of 50 mM Tris-HCl, 150 mM NaCl, 1% NP-40, 0.5% sodium deoxycholate, 2 mM sodium fluoride, 2 mM EDTA, 0.1% SDS, containing a mixture of protease inhibitors (aprotinin, phenylmethylsulfonyl fluoride, and sodium orthovanadate) for total protein extraction. Equal amounts of proteins were resolved on 11% SDS-polyacrylamide gel, transferred to a nitrocellulose membrane and probed with specific antibodies as described. To ensure equal loading, all membranes were stripped and incubated with anti- $\beta$  – Actin/GAPDH antibody. The antigen-antibody complex was detected by incubation of the membranes with peroxidase-coupled goat anti-mouse or goat anti-rabbit antibodies and revealed using the ECL System. Blots are representative of three independent experiments. The bands of interest were quantified by Scion Image laser densitometry scanning program and standard deviations along with associated P values for the biological replicates were determined by using GraphPad-Prism4 software.

**Transient transfection assays.** MCF-7 cells were transiently transfected using the FuGENE 6 reagent with either empty vector (e.v.) or FXR-DN plasmid for 24 h and then cells were treated as described. The FXR-DN expression plasmids were provided from Dr T.A. Kocarek (Institute of Environmental Health Sciences, Wayne State University, USA)<sup>53</sup>. RNA silencing. MCF-7 cells were transiently transfected with a siRNA targeted for the human SOCS3 RNA sequence (Qiagen, S103060358), or with a control siRNA (Qiagen, S100300650) to a final concentration of 30 nM using Lipofectamine 2000 as recommended by the manufacturer. After 24 h of transfection, cells were exposed to treatments.

**In vivo experiments.** The in vivo experiments were done in 45-day-old female athymic nude mice (Harlan Laboratories, Udine, Italy) maintained in a sterile environment. The animals were fully anesthetized by i.p. injection of chloral hydrate 400 mg/kg to allow the s.c. implantation of estradiol (E2) pellets (1.7 mg per pellet, 60-day release; Innovative Research of America, Sarasota, FL) into the intrascapular region. The day after, exponentially growing MCF-7 cells ( $5.0 \times 10^6$  cells per mouse) alone or in combination with CAFs were inoculated s.c. in 0.1 mL of Matrigel. In the group receiving both tumor cells and

CAFs, a ratio 3:1 (tumor cells/CAFs) was used. The subcutaneous location was used to eliminate the influence of other mammary gland cellular components on the interaction of human breast fibroblasts and epithelial cells. GW4064 treatment (30 mg/kg/day) was started when mean tumor size reaches to 100 mm<sup>3</sup> (day 0) and delivered daily to the animals by i.p. injection. Tumor development was followed twice a week by calliper measurements along two orthogonal axes: length (L) and width (W). The volume (V) of tumors was estimated by the following formula:  $V = L \times (W^2)/2$ . Relative tumor volume (RTV) was calculated from the following formula:  $RTV = (V_x/V_1)$ , where  $V_x$  is the tumor volume on day X and  $V_1$  is the tumor volume at initiation of the treatment. Growth curve was obtained by plotting the mean volume of RTV on Y axis against time (X axis expressed as days after starting of treatment). At day 32 the animals were sacrificed following the standard protocols and tumors were dissected from the neighboring connective tissue. Specimens of tumors were frozen in nitrogen and stored at  $-80\text{ }^{\circ}\text{C}$ . The remaining tumor tissues of each sample were fixed in 4% paraformaldehyde and embedded in paraffin for the histological analyses. All animals were maintained and handled in accordance with the

recommendation of the Guidelines for the Care and Use of Laboratory Animals and were approved by the Animal Care Committee of University of Calabria, Italy.

**Histopathological analysis.** Tumors, livers, lungs, spleens and kidneys were fixed in 4% formalin, sectioned at 5  $\mu$  m and stained with haematoxylin and eosin Y, as suggested by the manufacturer (Bio-Optica, Milan, Italy). Some sections from MCF-7/CAFs tumors were stained with Azan trichrome (Bio-Optica, Milan, Italy) to differentiate epithelial and connective components.

**Immunohistochemical analysis.** Paraffin-embedded sections, 5  $\mu$  m thick, were mounted on slides precoated with poly-lysine, and then they were deparaffinised and dehydrated (seven to eight serial sections). Immunohistochemical experiments were performed after heat-mediated antigen retrieval, using human Cytocheratin 18,  $\alpha$  SMA primary antibodies in MCF-7/CAF samples and FXR, Ki67, SOCS3, Ob, Survivin and Cyclin D1 primary antibodies in both MCF-7 and MCF-7/CAF samples at 4 °C overnight. Then, a biotinylated specific IgG was applied for 1 h at room temperature, followed by the avidin biotin horseradish peroxidase complex (Vector Laboratories, CA). Immunoreactivity was visualized by using the diaminobenzidine

chromogen (Sigma-Aldrich). Counterstaining was carried out with haematoxylin (Sigma-Aldrich). The primary antibody was replaced by normal serum in negative control sections. The immunostained slides of tumour samples were evaluated by light microscopy using the Allred Score<sup>54</sup>, which combines a proportion score and an intensity score. A proportion score was assigned representing the estimated proportion of positively stained tumor cells (0 = none; 1 = 1/100; 2 = 1/100 to < 1/10; 3 = 1/10 to < 1/3; 4 = 1/3 to 2/3; 5 = > 2/3). An intensity score was assigned by the average estimated intensity of staining in positive cells (0 = none; 1 = weak; 2 = moderate; 3 = strong). Proportion score and intensity score were added to obtain a total score that ranged from 0 to 8. A minimum of 100 cells were evaluated in each slide. Six to seven serial sections were scored in a blinded manner for each sample.

**Statistical analyses.** Each datum point represents the mean  $\pm$  S.D. of three different experiments. Data were analyzed by Student's t test using the GraphPad Prism 4 software program. For immunohistochemistry, the differences in the scores between GW-treated and vehicle-treated samples were examined by one-way ANOVA. \*P < 0.05 was considered as statistically significant.

---

# RESULTS

---

---

## **Activated FXR Inhibits Leptin-Induced Growth and Motility in Breast Cancer Cells.**

Leptin, acting in an autocrine, endocrine and paracrine manner, modulates many aspects of breast carcinogenesis from initiation and primary tumor growth to metastatic progression. Hence, our first aim was to investigate the role of activated FXR on leptin-induced cell proliferation and motility using as experimental models poorly invasive/low metastasizing MCF-7 estrogen receptor (ER)  $\alpha$  positive and highly invasive and metastatic MDA-MB-231 (ER $\alpha$  -negative) human breast cancer cells. Both MCF-7 and MDA-MB-231 cells were treated with leptin (500 ng/ml) with or without GW4064 (6 $\mu$  M), a synthetic FXR agonist, and growth was evaluated by anchorage-independent soft agar assays which closely mimic some in vivo biologic features of tumors. Leptin exposure increased colony numbers in both cell lines and this effect was completely reversed by GW4064 treatment (Fig. 1a). We then examined the ability of the FXR ligand to affect leptin-induced breast cancer cell movement in wound-healing scratch assays. Leptin-treated MCF-7 and MDA-MB-231 cells moved the farthest in either direction to close the gap compared to untreated cells, while GW4064 treatment was able to

significantly inhibit leptin-induced migration (Fig. 1b). Moreover, we also tested the effect of GW4064 in counteracting leptin-induced capacity of MCF-7 and MDA-MB-231 cells to invade an artificial basement membrane Matrigel in invasion assays. As showed in Fig. 1c, leptin-increased invasion of breast cancer cells was completely abrogated by GW4064 treatment.

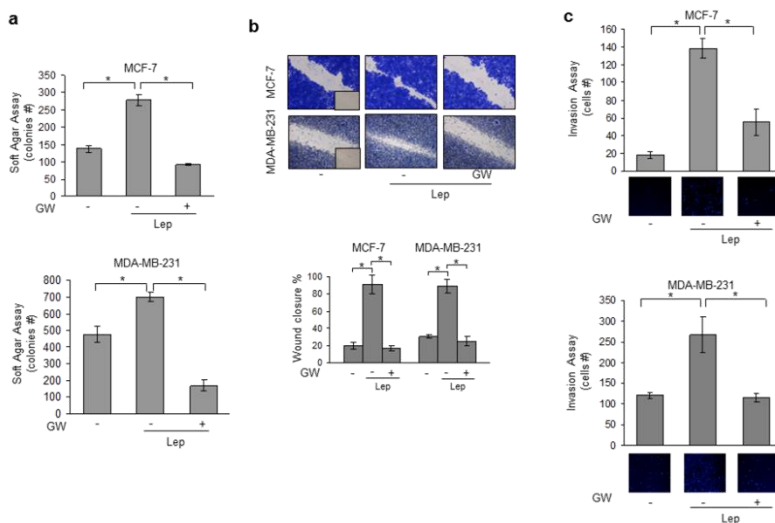


**Figure 1. Activated FXR Inhibits Leptin-Induced Growth and Motility in MCF-7 and MDA-MB-231 Breast Cancer Cells.** (a) Soft agar growth assays in MCF-7 and MDA-MB-231 cells treated with Leptin (Lep, 500 ng/ml) in the presence or absence of GW4064 (6  $\mu$  M). After 14 days of growth colonies >50  $\mu$ m diameter were counted. (b) Wound-healing assays in MCF-7 and MDA-MB-231 cells treated with Lep in the presence or absence of GW4064. Fields were photographed immediately after wounding (inset, time 0) and 24 or 12 hours later for MCF-7 and MDA-MB-231 cells, respectively. Upper panel, representative images from each condition are shown. Lower panel, the histograms represent the relative percentage of wound closure calculated by image analysis using Scion Image software. (c) Matrigel invasion assays in MCF-7 and MDA-MB-231 cells treated with Lep in the presence

or absence of GW4064. The migrated cells were 4',6-Diamidino-2-phenylindole (DAPI)stained, counted and images were captured at 10X magnification. Typical well for each condition is shown. The values represent the mean  $\pm$  SD of three different experiments, each performed in triplicate. \* $p < 0.05$ .

## GW4064 Reduces Leptin Signaling Pathway Activation and Leptin Target Gene Expression in Breast Cancer Cells.

Leptin exerts its biologic function through binding to its specific membrane receptor (ObR) able to activate multiple downstream signaling pathways (Sweeney G. *et al.*, 2002; Ahima R. *et al.*, 2004). First, we evaluated whether GW4064 treatment may affect the expression of leptin receptor (ObR) in breast cancer cells. As reported in Fig. 2, we did not observe any significant changes in ObR mRNA levels after treatment with GW4064 for 12 and 24 h.

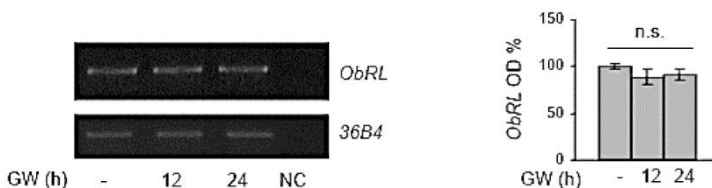


**Figure 2. Effects of Activated FXR on Leptin Receptor Expression in MCF-7 Breast Cancer Cells.**

Leptin receptor long isoform (ObRL) mRNA expression in MCF-7 cells treated for 12 or 24 hours with GW4064 (GW, 6 $\mu$ M) by RT-PCR analysis. 36B4(internal standard). NC, negative control. The histograms represent the mean  $\pm$  SD of three separate experiments in which band intensities were evaluated in terms of optical density arbitrary units (OD) and expressed as percentage of vehicle-treated samples which were assumed to be 100%; n.s.:nonsignificant.

Then, immunoblot analysis was performed to evaluate the phosphorylation levels of the major leptin downstream signaling molecules in cells pretreated or not with GW4064 for

12 h and then subjected to short-term stimulation with leptin. As expected, in both MCF-7 and MDA-MB-231 cells, leptin treatment resulted in increased phosphorylation levels of JAK2, STAT3, AKT and MAPK compared to untreated cells, whereas pretreatment with GW4064 abrogated the leptin activation of these signaling pathways (Fig. 3a). Next, we evaluated the impact of activated FXR on the expression of well-known leptin target genes, such as Ob, Cyclin D1 and Survivin (*Saxena N.K. et al., 2007; Chen C. et al., 2006; Catalano S. et al., 2009; Jiang H. et al., 2008; Catalano S. et al., 2011; Knight B.B. et al., 2011*). We observed that exposure to GW4064 significantly reduced leptin induction on ObR mRNA levels (Fig. 3b) as well as leptin-mediated upregulation of Cyclin D1 and Survivin protein content (Fig.3c) in both MCF-7 and MDA-MB-231 cells. These effects were completely reversed in cells transiently transfected with a dominant negative FXR (FXR-DN) plasmid, supporting the direct involvement of this nuclear receptor in affecting leptin signaling in breast cancer cells (Fig.3d).

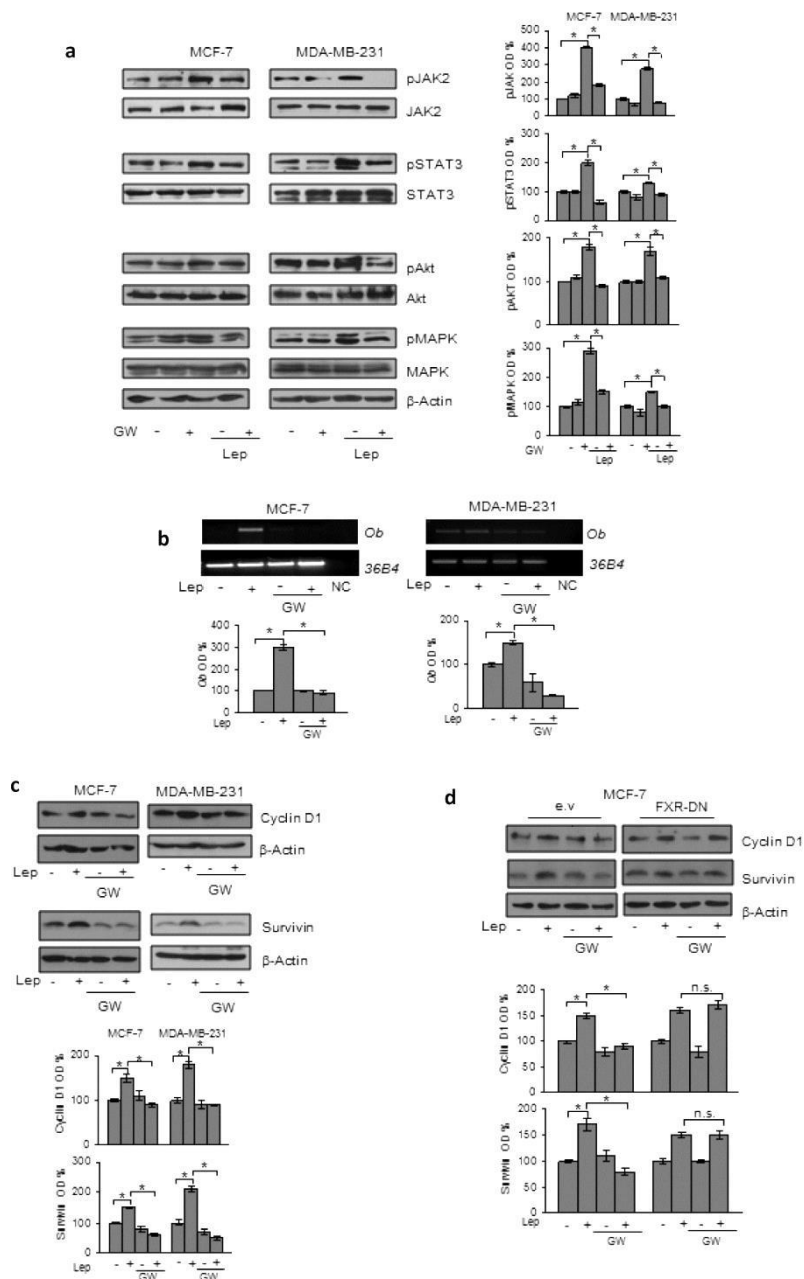


**Figure 3. Effects of GW4064 on Leptin Signaling and its Target Genes in Breast Cancer Cells.**

(a) MCF-7 and MDA-MB-231 cells were pretreated for 12 h with GW4064 and then treated or not for 10 min with Lep. Levels of phosphorylated (p) JAK2, STAT3, Akt, and MAPK, and total non-phosphorylated proteins were evaluated in cellular extracts by immunoblot analysis.  $\beta$ -Actin was used as loading control. (b) Total RNA was extracted from MCF-7 and MDA-MB-231 cells, pretreated for 12 h with GW4064 and then treated or not for 24 h with Lep, reverse transcribed and cDNAs were subjected to PCR using primers specific for Ob or 36B4 (internal control). NC: negative control. (c) Immunoblot analysis for Cyclin D1 and Survivin expression in MCF-7 and MDA-MB-231 cells pretreated for 12 h with GW4064 and then treated or not for 24 h with Lep. (d) MCF-7 cells were transiently transfected with either empty vector (e.v.) or FXR dominant negative plasmid (FXR-DN), pretreated for 12 h with GW4064 and then treated or not for 24 h with Lep. Cyclin D1 and Survivin expression levels were evaluated by immunoblotting.  $\beta$ -Actin was used as loading control. The histograms represent the mean  $\pm$  SD of three separate experiments in which band intensities were evaluated in terms of optical density arbitrary units (OD) and expressed as percentage of vehicle-treated samples which were assumed to be 100%. n.s. = non-significant, \* $p < 0.05$ .

The suppressor of cytokine signaling 3 (SOCS3), the negative feedback regulator of leptin receptor signaling pathway (Croker B.A. *et al.*, 2008; Cirillo D. *et al.*, 2008) has been recently identified as a direct FXR target gene (Xu Z. *et al.*, 2012; Li G. *et al.*, 2013). Thus, to gain insights into the molecular mechanism underlying the inhibitory role of activated FXR on leptin transductional pathways, we conducted time-course studies to examine the effects of the FXR ligand on the expression of SOCS3 in MCF-7 cells. Treatment with GW4064 was able to increase the cellular content of SOCS3 at both mRNA and protein levels (Fig.4a, b). The direct involvement of activated FXR in the regulation of

SOCS3 expression in breast cancer cells was ascertained by evaluating SOCS3 content in the presence of FXR-DN plasmid. As shown in Fig.4c, the expression of the FXR-DN completely abrogated the GW4064-induced SOCS3 levels. Finally, the functional relevance of SOCS3 in mediating GW4064 effects was confirmed by knocking-down its expression in MCF-7 cells (Fig.4d). SOCS3 gene silencing abolished the inhibition exerted by GW4064 on leptin-induced effects on downstream signaling molecules, such as MAPK and Survivin (Fig.4e). Taken together, these data demonstrate that modulation of SOCS3 expression may represent a mechanism through which FXR activation could affect leptin activity on breast cancer.

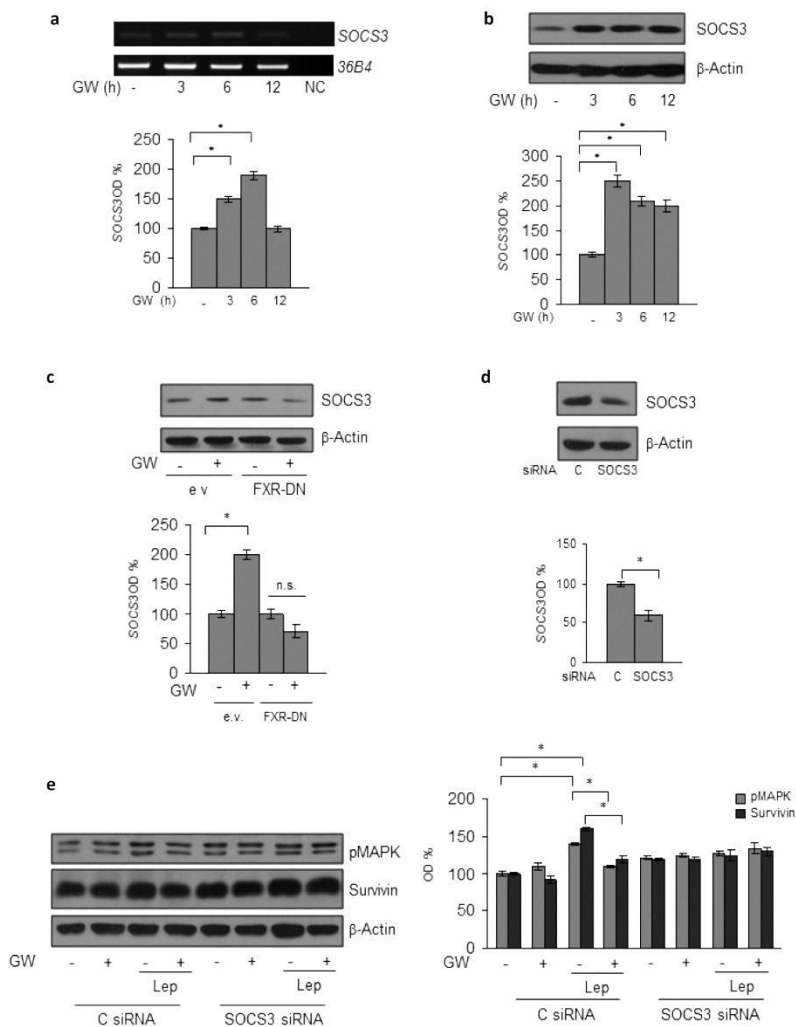


**Figure 4. SOCS3 Mediates GW4064 Effects on Leptin Signaling Molecules in MCF-7 Breast Cancer Cells.**

(a) Total RNA was extracted from MCF-7 cells treated with GW4064 as indicated, reverse transcribed and cDNAs were subjected to PCR using primers specific for SOCS3 or 36B4 (internal control). NC: negative control. Immunoblotting analysis for SOCS3 expression in total protein extracts from MCF-7 cells treated with GW4064

as indicated **(b)** or from MCF-7 cells transiently transfected with either empty vector (e.v.) or FXR dominant negative plasmid (FXR-DN) and treated with GW4064 **(c)** or from MCF-7 cells transiently transfected with either a control siRNA (C siRNA) or a siRNA targeted for the human SOCS3 RNA sequence (SOCS3 siRNA) **(d)**. **(e)** Levels of phosphorylated (p) MAPK and Survivin were evaluated in protein extracts from MCF-7 cells transfected and treated as indicated by immunoblot analysis.  $\beta$  - Actin was used as a loading control. The histograms represent the mean  $\pm$  SD of three separate experiments in which band intensities were evaluated in terms of optical density arbitrary units (OD) and expressed as percentage of vehicle-treated samples which were assumed to be 100%. n.s. =non-significant; \* $p < 0.05$ .

### **GW4064 Reverses CAF-Induced Breast Cancer Cell Growth and Motility**

Recently, we have identified leptin as one of the most important molecular player that mediates CAF effects in influencing tumor cell behavior. Indeed, we used CAFs isolated from biopsies of primary breast tumors. CAFs possessed the basic fibroblast characteristics with long and spindle-shaped morphology and highly expressed alpha-smooth muscle actin ( $\alpha$ -SMA), vimentin, and fibroblast activation protein (FAP) (Fig. 5a, b).

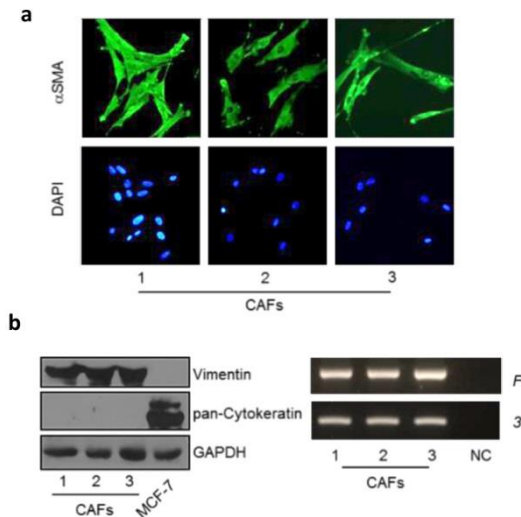


**Figure 5. Characterization of Cancer Associated Fibroblasts (CAFs) Used in this Study.**

(a) CAFs were isolated from primary breast tumour biopsies by collagenase digestion. Immunofluorescence of alpha-smooth muscle actin ( $\alpha$ -SMA) and DAPI staining (for nuclei detection). (b) Left panel, immunoblotting of Vimentin and pan-Cytokeratin protein expression, GAPDH as loading control. Right panel, RT-PCR analysis of Fibroblast Activation Protein (FAP) mRNA levels. 36B4 (internal standard). NC, negative control.

Moreover, we have shown that leptin immunodepletion from CAF-derived conditioned media (CAF-CM) substantially reduced the growth- and migration-promoting activities of CAFs on breast cancer cells (*Barone I. et al., 2012*). On the basis of these data and since the activated fibroblasts are the principal cellular components in the breast stromal compartment, we investigated the ability of GW4064 to interfere with tumor microenvironment pressure. Indeed,

ELISA measurement in conditioned media from CAFs confirmed leptin secretion ( $2,6 \pm 0,21$  ng/ mg protein). Both MCF-7 and MDA-MB-231 cells were incubated with CAF-CM and growth was evaluated by anchorage-independent soft agar assays. CAF-CM significantly enhanced colony numbers in both cell lines and treatment with GW4064 effectively counteracted the CAF-elicited increase in tumor cell growth (Fig. 6a). Then, we investigated the ability of the FXR ligand to inhibit the effects of conditioned media from CAFs on cell migration and invasion in MCF-7 and MDA-MB-231 cells. As shown in Fig. 6b, CAF-CM significantly accelerated closure of the cell-cleared area in both cell lines compared to control media, and GW4064 treatment was able to reverse these effects. Moreover, CAF-CM stimulation also increased the number of invaded cells in both cell lines and as expected treatment with GW4064 resulted in a clear reduction of cell invasion induced by CAF-CM (Fig. 6c).

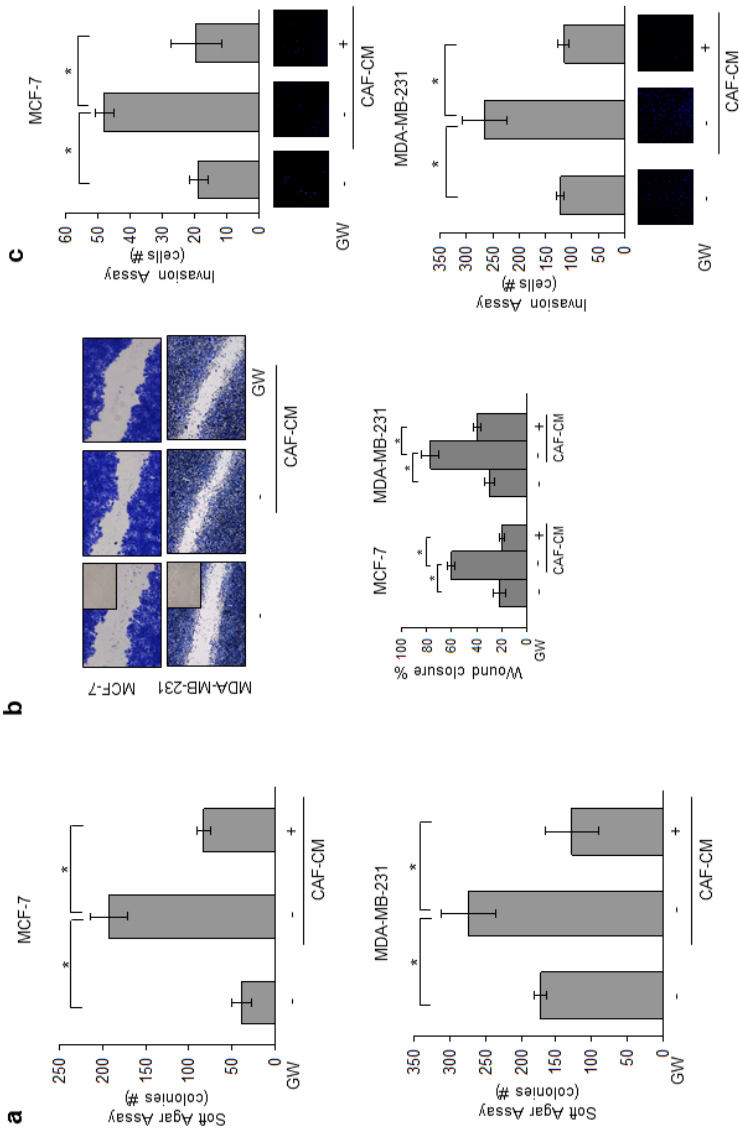


**Figure 6. GW4064 Effects on CAF Conditioned Media-Induced Growth and Motility in Breast Cancer Cells.**

(a) Soft agar growth assays in MCF-7 and MDA-MB 231 cells treated with CAF-derived conditioned media (CAF-CM) in the presence or absence of GW4064. (b) Wound-healing assays in cells treated as indicated. Fields were photographed immediately after wounding (inset, time 0) and 24 or 12 hours later for MCF-7 and MDA-MB-231 cells, respectively. Upper panel, representative images from each condition are shown. Lower panel, the histograms represent the relative percentage of wound closure calculated by image analysis using Scion Image software. (c) Matrigel invasion assays in cells treated as indicated. The migrated cells were DAPI stained, counted and images were captured at 10X magnification. Typical well for each condition is shown. The data represent the mean  $\pm$  SD of three independent experiments, each performed in triplicate. \* $p < 0.05$ .

**Impact of FXR activation in SKBR3 breast cancer cells.**

We also evaluated the effects of activated FXR in interfering with leptin actions in ER- $\alpha$  negative and HER2 overexpressing SKBR3 breast cancer cells. As expected, our results clearly show that FXR activation affected leptin stimulatory effects on growth, motility and invasiveness of SKBR3 cell model (Fig. 7a, 7b). In addition, GW4064 was able to negatively regulates leptin-target genes as showed in Fig. 7c and 7d. We also demonstrated that GW4064 significantly reduced SKBR3 cell proliferation and motility mediated by exposure with CAF-CM (Fig. 7e and 7f). All together, these results clearly show that FXR activation affects leptin stimulatory effects and cancer promoting activities of CAF on growth, motility and invasiveness in different breast cancer cell models.

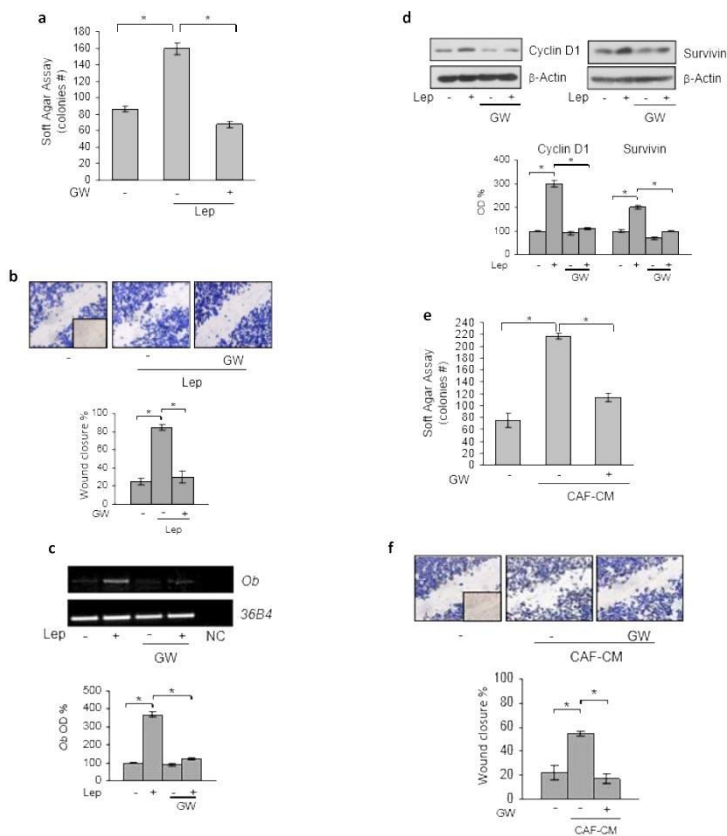


**Figure 7. Effects of Activated FXR in SKBR3 Breast Cancer Cells.**

(a) Soft Agar growth assay in SKBR3 cells treated with Leptin (Lep, 500ng/ml) with/without GW4064 (6 $\mu$ M). (b) Wound-healing assay in cells treated as indicated for 24h. Upper panel, representative images from each condition (inset, time 0). Lower panel, relative percentage of wound closure. (c) RT-PCR analysis of leptin (Ob) mRNA levels. 36B4, internal standard. NC, negative control. (d) Immunoblot analysis for Survivin, Cyclin D1,  $\beta$ -Actin (loading control) expression. Lower panels for (c) and (d), the histograms represent the mean  $\pm$  SD of three separate experiments in which band intensities were evaluated in terms of optical density arbitrary units (OD), expressed as percentage of vehicle-treated samples assumed to be 100%. (e) Soft Agar growth assay in cells treated with CAF-CM with/without GW4064. (f) Wound-healing assay in cells treated as indicated. Upper panel, representative images from each condition (inset, time 0). Lower panel, relative percentage of wound closure. The values represent the mean  $\pm$  SD of three independent experiments. \* $p < 0.05$ .

**The FXR ligand GW4064 Inhibits Tumor Growth in MCF-7/CAF xenografts.** Based on our results demonstrating that FXR activation may counteract tumor-promoting ability of CAFs in vitro, we used mouse xenograft models to examine the effect of GW4064 on breast cancer growth in vivo. Hence, MCF-7 cells were injected alone or in combination with CAFs into the intrascapular region of female nude mice and tumor growth was monitored upon the administration of vehicle or 30 mg/kg/die GW4064. This treatment was well tolerated because no change in body weight or in food and water consumption was observed, along with no evidence of reduced motor function. In addition, no significant differences in the mean weights or histological features of the major organs (liver, lung, spleen, and kidney) after sacrifice were observed between vehicle-treated mice and those that received treatment, indicating a lack of toxic effects at the dose given. Tumor volume was measured from the first day of treatment and the relative tumor volume was calculated as described in detail in Materials and Methods. As shown in Fig. 8a, the co-injection of MCF-7 cells with CAFs determined an impressive acceleration in tumor growth when compared to MCF-7 alone. Importantly, GW4064 treatment induced a

significant regression in tumor growth in both groups, even though in higher extent in MCF-7/CAF group. To differentiate epithelial and connective components, MCF-7/CAF samples were stained with hematoxylin and eosin or Azan trichrome stain (Fig. 8b, c, respectively). The same sections were also incubated with anti-human- $\alpha$  SMA and anti-human-Cytokeratin 18 antibodies to verify the human origin of epithelial and connective analyzed tissues (Fig. 8d).

Immunostaining of FXR in sections of tumors obtained from GW4064-treated mice revealed an increased immunoreactivity of this receptor, respect to mice treated with vehicle, consistently with the FXR activation by its own ligand (Fig. 9a and Table 2). Moreover, in agreement with our in vitro findings, we observed in xenograft tumors from mice treated with GW4064 a significant reduction in the expression of Ki67, a well-known marker for cell proliferation (Fig. 9a and Table 2). Interestingly, in GW4064-treated tumors we showed a strong intensity staining for SOCS3 along with a marked decrease in the expression of Survivin, Cyclin D1, and Ob (Fig. 9a and Table 2). The up-regulation of FXR and SOCS3 was further validated by RT-PCR analysis on tumor tissue samples (Fig. 9b). Moreover, we revealed no significant changes in Ob

mRNA levels among vehicle- and GW4064-treated samples (Fig. 9b), suggesting that a different regulation on Ob mRNA and protein levels may occur after GW4064 treatment.

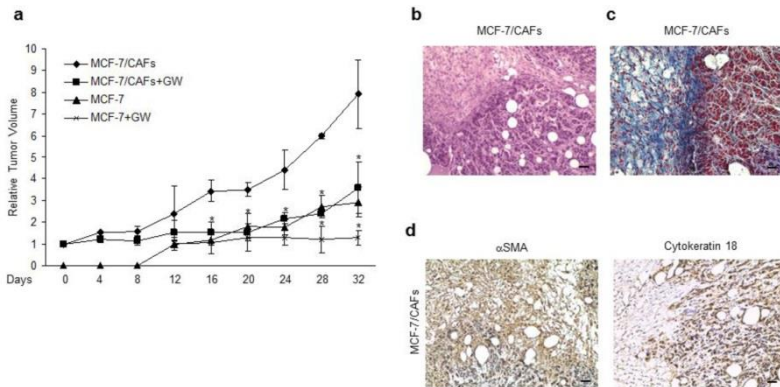


**Figure 8. Impact of GW4064 Treatment on Tumor Growth of MCF-7 and MCF-7/CAF Xenografts.**

(a) MCF-7 cells were injected alone or coinjected with CAFs (MCF-7/CAFs) subcutaneously into nude mice (5 mice/each group). GW4064 treatment (30 mg/kg/day) was started when tumor size reaches to 100 mm<sup>3</sup> (day 0, MCF-7/CAFs group; day 12, MCF-7 group) and delivered daily to the animals by i.p. injection. Relative tumor volume (RTV) was calculated from the following formula:  $RTV = (V_x/V_1)$ , where  $V_x$  is the tumor volume on day  $X$  and  $V_1$  is the tumor volume at initiation of the treatment for each group. Y axis: the mean and  $\pm$  SD of the RTV. \* $p < 0.05$ , GW4064-treated versus vehicle-treated animals. (b) Representative Hematoxylin and Eosin (H&E) and (c) Azan trichrome stained histologic images of MCF-7/CAF xenograft tumors (20X). (d) Human  $\alpha$  SMA (left panel) and Cytokeratin 18 (right panel) immunohistochemical staining of MCF-7/CAF xenograft tumor sections. Scale bars = 25  $\mu$  m.

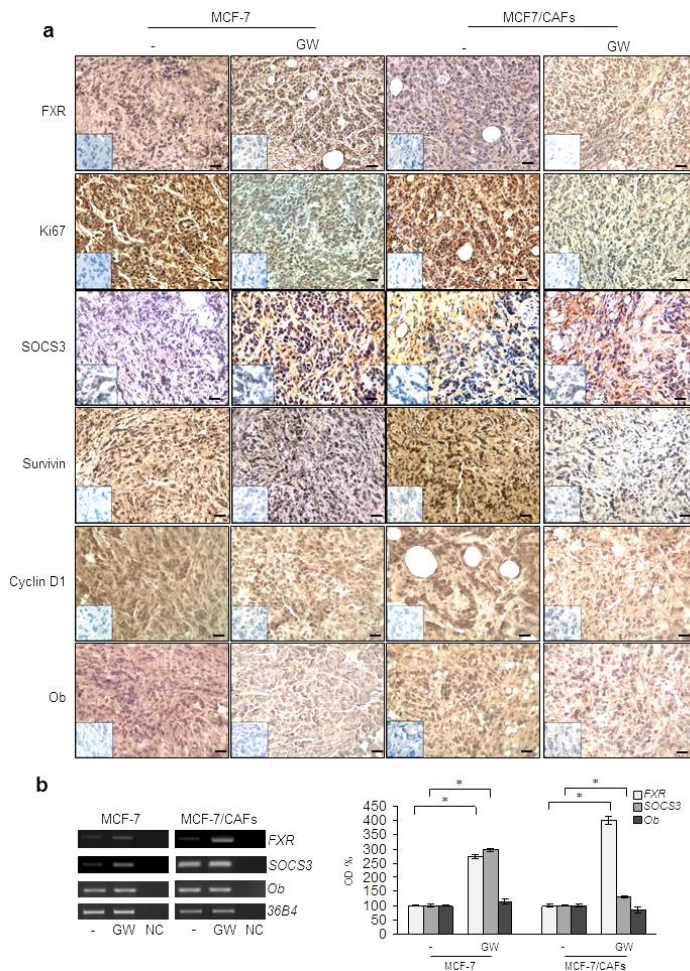


**Figure 9. GW4064 Decreases Leptin Target-Genes Expression in Xenograft Tumors.**

(a) Representative pictures of FXR, Ki67, SOCS3, Survivin, Cyclin D1 and Ob immunohistochemical staining of MCF-7 and MCF-7/CAF xenograft tumors. Inset: negative control. Scale bars = 25  $\mu$  m. (b) Total RNA from xenografts excised from vehicle and GW4064-treated mice was reverse transcribed and cDNA was subjected to PCR for expression of FXR, SOCS3, Ob and 36B4 (internal standard). NC: negative control. The histograms represent the mean  $\pm$  SD of separate tumor samples in which band intensities were evaluated in terms of optical density arbitrary units (OD) and expressed as percentage of vehicle-treated samples which were assumed to be 100%. \* $p < 0.05$ .

**Table 2. Immunohistochemistry Scores in MCF-7 and MCF-7/CAF Xenograft Tumors.**

Note: Cases were scored according to Allred immunohistochemistry (IHC) score<sup>54</sup> which includes both the proportion and intensity scores (range, from 0 to 8). \*P <0.001 GW4064-treated versus vehicle-treated samples. FXR: Farnesoid X Receptor; SOCS3: Suppressor of cytokine signaling 3; Ob: Leptin.

Antibody	IHC score in tumor cells			
	MCF-7		MCF-7/CAFs	
	-	GW4064	-	GW4064
FXR	4	6*	3	6*
Ki67	8	2*	8	2*
SOCS3	1	5*	2	6*
Survivin	5	2*	6	1*
Cyclin D1	6	5*	7	4*
Ob	5	3*	4	2*

All these results, highlighted the ability of activated FXR to counteract not only leptin signaling, responsible for mammary carcinogenesis, but also to affect the tumor promoting activities of CAFs within the breast microenvironment. Thus, we addressed to investigate whether FXR agonist may influence CAF phenotype.

### **FXR Expression and Activation in CAFs.**

CAFs, the most prevalent cellular component of the breast tumor microenvironment, are actively involved in tumor initiation and progression. To examine the potential role of activated FXR in influencing the behavior of CAFs, we first evaluated the expression of Farnesoid X Receptor in seven

different CAFs. As shown in Fig.10a, qRT-PCR analysis demonstrated the presence of FXR mRNA in all CAFs tested. The expression of FXR was then confirmed by evaluating protein levels using immunoblotting (Fig.10b) and immunofluorescent staining (Fig.10c). MCF-7 cell line was used as a positive control for FXR expression. Then, we evaluated the impact of activated FXR on the mRNA expression of well-known FXR target genes, such as SHP (Small Heterodimer Partner, SHP) and BSEP (Bile Salt Export Pump, BSEP). As expected we observed that CAFs, after treatment with GW 4064 for 24 hours, showed a significant up-regulation in SHP and BSEP mRNA expression levels (Fig.10d). All together, these data indicated, for the first time, that FXR is expressed in CAFs.

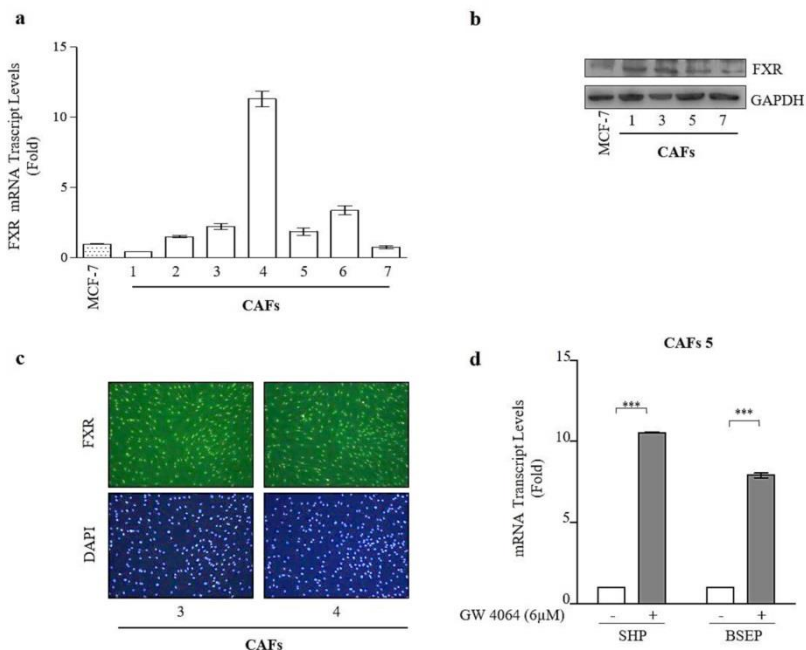


**Figure 10. FXR Characterization and Activity in CAFs.**

(a) qRT-PCR analysis for FXR mRNA levels in CAFs. Each bar represents mRNA expression relative to GAPDH mRNA (endogenous control gene)  $\pm$  S.D. (average of three samples). (b) Immunoblotting for FXR expression in indicated experimental models.  $\beta$ -actin, control for loading. (c) Immunofluorescence microscopic analysis to visualize FXR expression and localization in CAFs. Representative images of 2 CAFs are shown. (d) qRT-PCR analysis to evaluate mRNA expression levels of SHP (Small Heterodimer Partner) and BSEP (Bile Salt Excretory Pump), two FXR target genes, in CAFs treated for 24 hrs with vehicle (-) or the selective synthetic FXR agonist GW4064 (GW, 6  $\mu$ M). Each bar represents mRNA expression relative to GAPDH mRNA (endogenous control gene)  $\pm$  S.D. (average of three samples). \*\* $p < 0.001$ , \*\*\* $p < 0.0001$ .

---

**Impact of Activated FXR on Motility and Proliferation in CAFs.**

We next assessed whether GW 4064 treatment may cause any changes in CAF phenotype, including proliferation and migration. As shown in Fig.11a, anchorage-dependent growth assays revealed that GW 4064 exposure did not affect CAF proliferation. Then, we evaluated the ability of activated FXR to promote cell migration in wound-healing scratch assays and found that GW 4064 treatment was able to reduce the capability of CAFs to close in either direction the gap compared to untreated cells (Fig.11b). To extend the results obtained, the effects of GW 4064 on CAF migration ability were further confirmed by transmigration assay. Again, activated FXR was associated with a significant reduction of CAF motility (Fig.11c). Furthermore, to validate the direct involvement of FXR activation in the modulation of CAF behavior, we evaluated the biological effect of Guggulsterone, a natural FXR selective antagonist. Our data clearly demonstrated that the co-treatment with GW 4064 and Guggulsterone was able to reverse the effect deriving from FXR activation on CAF motility. Taken together, these data demonstrate that ligand-mediated activation of FXR is able to modulate motility of CAFs, without influencing their proliferative capabilities.

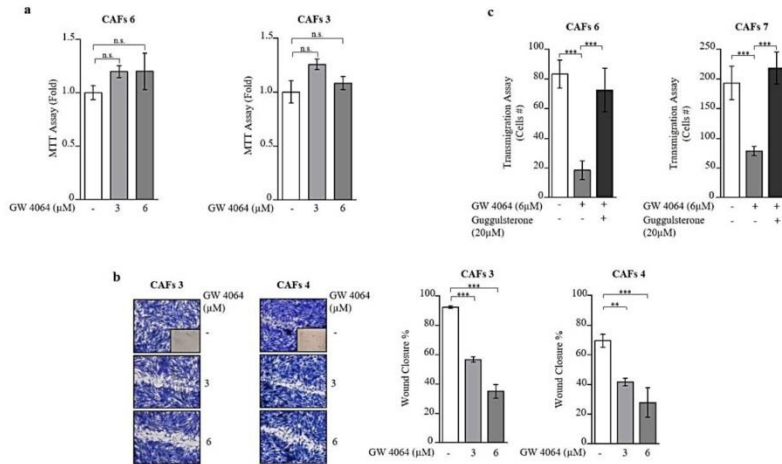


**Figure 11. Activated FXR Impact on CAFs Proliferation and Motility.**

(a) Anchorage-dependent MTT growth assays in two different CAFs treated in the presence or not with GW 4064 (GW, 3-6 μM) for 72 hrs. n.s., nonsignificant. (b) Cells were subjected to *in vitro* scratch assay with images captured at 0 and 24 hrs after incubation with vehicle (-) or GW4064 (3 and 6 μM). Small squares, time 0. *Left panel*, pictures are representative of three independent experiments. *Right panel*, the histograms represent the relative percentage of wound closure calculated by ImageJ software. \* $P < 0.05$ , \*\* $P < 0.001$ , \*\*\* $P < 0.0001$ . (c) Boyden-Chamber Transmigration Assay was used to evaluate the motility in CAFs treated with vehicle (-) or GW4064 (GW, 6 μM) and Guggulsterone (20 μM). After 24 hrs, migrated cells were fixed and stained with DAPI. Migration was quantified by viewing five separate fields per membrane at 10X magnification and expressed as the mean number of migrated cells in three-independent experiments.

## GW 4064-treated CAFs Exhibit a Reduction in the Activity of Rho GTPase and Integrin Signaling.

Since activated FXR significantly influenced CAF motility, to gain insight into the molecular mechanism responsible for these effects, quantitative transcriptome profiling of vehicle- and GW 4064 -treated CAFs was carried out by RNA-

sequencing analysis. Comparison of the whole transcriptome of untreated and treated CAFs revealed 873 differentially expressed genes (FDR<0.05), of which 577 were down-regulated and 199 up-regulated in response to GW 4064 treatment (Fig.12a). These genes were then subjected to Ingenuity Pathway Analysis (IPA) to rank enriched biologic processes, and to determine the activation z-score of molecular and cellular functions and pathways. In line with our previous experiments, cellular movement was the most significantly down-regulated biologic process in GW 4064 - treated CAFs (Fig. 12b). Interestingly, analysing the functions involving differentially expressed genes, migration and movement resulted to be highly reduced by GW 4064 treatment (Fig. 12c). Then, considering the most affected pathways by FXR activation in CAFs, we found marked changes in the activity of Rho GTPase family and Integrin signaling, with activation z-score of -1, -0,5 respectively (Fig. 12d). These results are in agreement with the reduced migration mediated by activated FXR in CAFs, since these proteins are known to govern cell cytoskeleton organization and migration. To confirm the gene expression profile obtained by RNA sequencing analysis, we compared expression and activation

of Rho family proteins in vehicle- and GW 4064- treated CAFs. A significant reduction in protein levels of Cdc42, Rho A-C, Rac1-3 and p-Miosin (Fig.13a) were detected in GW 4064-treated cells. Furthermore, to deepen the role of Rho proteins activation on cytoskeletal organization in our model systems, we evaluated the formation of stress fibers, as they provide the contractile force required for motility (Fig. 13b). In vehicle-treated cells, actin fibers were clearly visible and diffusely distributed in the cytoplasm, while GW 4064 treatment resulted in a visible reduction of stress fibers. Our data further showed that the molecular and cellular functions identified with IPA are biologically relevant and activated FXR may regulate motility and migration of CAFs through the involvement of Rho proteins family.

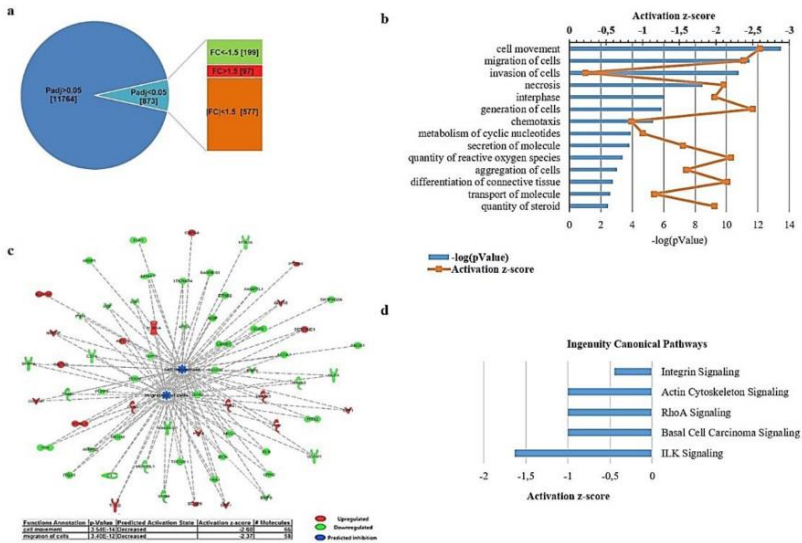


**Figure 12. Biologic Processes, Functions, and Pathways Identified from RNA Sequencing Data in GW 4064-Treated CAFs.**

Ingenuity Pathway Analysis (IPA) was used to identify functions and pathways significantly associated with differentially-expressed genes (a) and to calculate activation z-score of biological pathways (b) in CAFs treated with GW4064 (6  $\mu\text{M}$ , 24 hrs) compared to CAFs treated with vehicle. IPA identify most affected functions for all highly down-regulated genes in CAFs treated with vehicle or GW4064 for 24 hrs (c) and pathways (d), highlighting a significant down-regulation of genes involved in Integrin Signaling Pathway and in Rho Signaling Pathway in GW-treated CAFs.

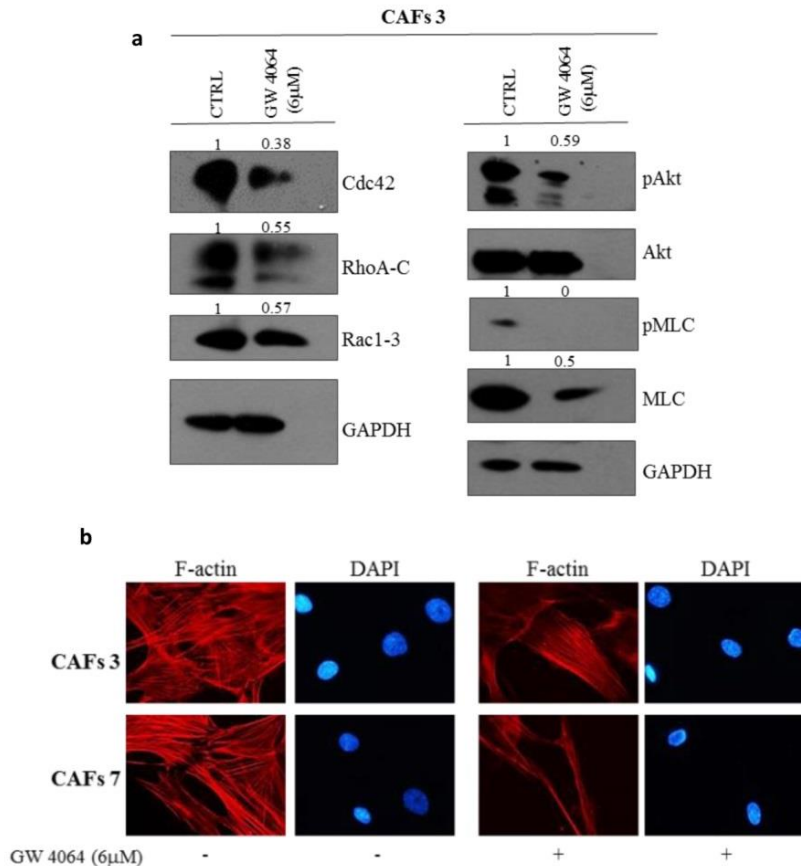


**Figure 13. Rho Proteins Cascades in GW 4064-Treated CAFs.**

(a) Immunoblotting for Cdc42, Rho A-C, and Rac 1-3 expression and phosphorylated myosin light chain (pMLC<sup>Thr18/Ser19</sup>) and total proteins from whole cell lysates. GAPDH, control for loading. (b) Phalloidin staining of F-actin (stress fibers, red) in CAFs treated with GW 4064 for 24hrs. DAPI, nuclear staining.

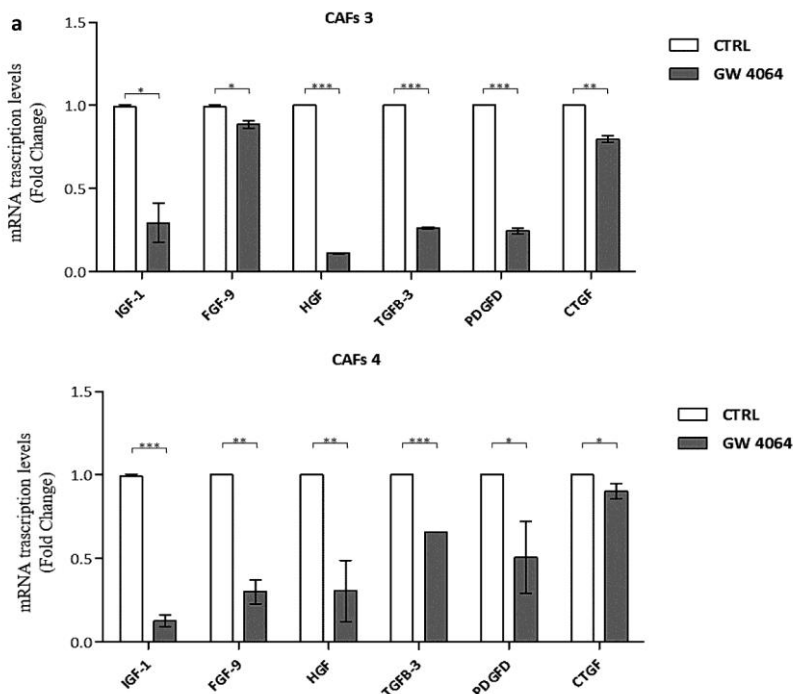


**Figure 14. GW 4064 Reduced CAFs Secreted Factors.**

(a) qRT-PCR analysis to evaluate mRNA expression levels of IGF-1 (Insulin Growth Factor-1), FGF-9 (Fibroblast Growth Factor-9), HGF (Hepatocyte Growth Factor), TGFβ-3 (Transforming Growth Factor β-3), PDGFD (Platelet Derived Growth Factor D) and CTGF (Connective Tissue Growth Factor), in CAFs treated for 24 hrs with vehicle (-) or the selective synthetic FXR agonist GW4064 (GW, 6 μM). Each bar represents mRNA expression relative to GAPDH mRNA (endogenous control gene) ± S.D. (average of three samples). \* $P < 0.05$ , \*\* $P < 0.001$ , \*\*\* $P < 0.0001$ .

### **GW 4064 treatment reduced secretion of CAF soluble factors.**

Diffusible growth factors, interleukins, chemokines secreted mainly by CAFs, as mediators of stromal-epithelial interactions, play a crucial role in supporting breast

tumorigenesis. Gene expression profiling revealed that FXR activation in CAFs was able to reduce expression of different secreted soluble factors (Table 3). Data obtained from RNA-seq were also validated through qRT-PCR analysis (Fig. 14). Our results clearly demonstrated that GW 4064 treatment in CAFs is able to significantly reduce several secreted factors, that represented key players in the maintenance of cancer growth and progression.

**Table 3.** RNA-sequencing was used to analyze changes in gene expression of the different factors secreted by CAFs treated with vehicle and GW4064 and potentially involved into tumor-stroma interactions.

<i>Gene Name</i>	<i>Gene Symbol</i>	<i>Fold Change in GW-treated CAFs</i>	<i>p-value</i>
Insulin Like Growth Factor 1	<i>IGF1</i>	-2,412425888	5,30E-12
Fibroblast Growth Factor 9	<i>FGF9</i>	-1,934906657	1,85E-07
Hepatocyte Growth Factor	<i>HGF</i>	-1,761911618	3,45E-06
Transforming Growth Factor Beta 3	<i>TGF-<math>\beta</math></i>	-1,453924778	0,000550842
Platelet Derived Growth Factor D	<i>PDGFD</i>	-1,382536341	0,002860403
<u>Connective Tissue Growth Factor</u>	<i>CTGF</i>	-1,341551235	0,000529047
C-X-C Motif Chemokine Ligand 5	<i>CXCL5</i>	-1,341152562	0,002854343
Interleukin 6	<i>IL6</i>	-1,340950913	0,000768066
C-C Motif Chemokine Ligand 2	<i>CCL2</i>	-1,270802933	0,001599915
C-X-C Motif Chemokine Ligand 12	<i>CXCL12</i>	-1,234858064	0,003102473
Fibroblast Growth Factor 14	<i>FGF14</i>	-1,227215567	0,003184261

**Effects of GW 4064-treated CAFs on Breast Cancer Phenotype.**

As a final step of this study, we defined the effects of conditioned media from GW 4064 treated CAFs on breast cancer cell behavior. To this aim, co-culture experiments were performed with CAFs and two breast cancer cell lines ER $\alpha$  - positive MCF-7 and T47D. Exposure to conditioned media derived from CAFs treated with GW 4064 (6 $\mu$ M) for 24 hours significantly reduced growth by anchorage-independent soft agar assay (Fig.15a). We then examined the ability of GW 4064-treated CAFs on cell migration in MCF-7 and T47D cells. As shown in Fig.15b, GW4064 treatment was able to reduce cell proliferation induced by CM-CAF. Furthermore, Soft Agar and Transmigration assays on the above described co-culture models (Fig.15c, d) demonstrated that exposure with an FXR antagonist, Guggulsterone, was able to reverse the effects deriving from FXR activation, supporting the direct involvement of this nuclear receptor in modulating CAF activities. Collectively, these results highlight the ability of activated FXR to counteract tumor-promoting of CAFs on breast cancer cell lines.

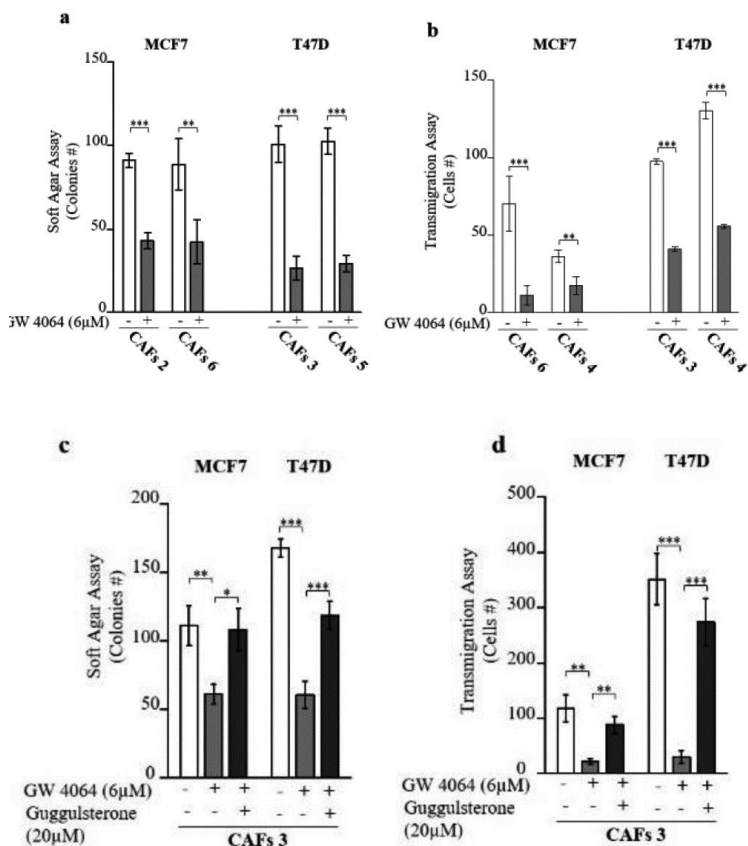


**Figure 15. Effect of GW 4064 on Breast Cancer Cells.** CAFs were treated with vehicle (-) or with GW4064 (GW, 6μM). After 24 hrs, conditioned media were collected and used for (a) Soft Agar growth assay in co-culture experiments with human Estrogen Receptor-positive MCF-7 and -negative T47D breast cancer cells. After 14 days of growth, colonies > 50 μm diameter were counted. The values represent the means ± SD of three different experiments each performed in triplicate. \*\* $P < 0.001$ , \*\*\* $P < 0.0001$ . (b) Boyden-Chamber Transmigration Assay was used to evaluate the motility of MCF-7 and T47D breast cancer cells, after 24 hr of incubation with conditioned media derived from CAFs treated with vehicle (-) or GW4064 (GW, 6 μM). \*\*\* $P < 0.0001$ .

Co-culture experiments with MCF-7 and T47D breast cancer cells in presence of CM derived from CAFs treated with vehicle (-) or with GW4064 (GW, 6μM) in presence or absence of Guggulsterone (20 μM), was used to perform (c) Soft Agar assay and (d) Boyden-Chamber Transmigration Assay. \*\* $P < 0.001$ , \*\*\* $P < 0.0001$ .

---

## DISCUSSION

---

The stromal cells located within the tumor microenvironment are now extensively recognized to directly influence the malignant features of adjacent tumor cells. Interactions between tumor cells and the associated stroma represent a solid relationship that impacts disease initiation, progression and patient prognosis (*Hanahan D. et al., 2011; Quail D.F. et al., 2013*). Emerging evidences have proposed cancer associated fibroblasts (CAFs) as a pivotal cell type able to shape the architecture of the microenvironment and modulate communications between the various cell types present in the tumor through several signaling molecules, such as growth factors, extracellular matrix-degrading proteases, chemokines and cytokines (*Aboussekhra A. et al., 2011*). Of note, activated stromal fibroblasts have been shown to promote carcinogenesis both in vitro and in animal models and an high number of CAFs are often associated with high-grade malignancies and poor prognosis (*Aboussekhra A. et al., 2011; Luo H. et al., 2015; Mao Y. et al., 2013*). Therefore, a better understanding of the epithelial-stromal interactions has the potential to identify novel therapeutic targets for developing more effective anticancer approaches. Here, we evidenced, for the first time, that activated FXR, by interfering

with the tumor supportive effects of CAFs, is able to inhibit breast cancer growth, motility and invasion. Particularly, we demonstrated that the specific FXR ligand, GW4064, affects the signaling of the adipokine leptin that we have recently identified as one of the most important molecules involved in the tumor-promoting activity of CAFs in breast cancer cells (*Barone I. et al., 2012*). Our results showed that GW4064 restrains the leptin-induced growth, motility, and invasiveness in both ER $\alpha$  -positive and -negative breast cancer cells. The anti-tumor action of the FXR ligand was associated with the inhibition of several leptin-induced pathways, such as JAK2/STAT3, AKT and MAPK. Interestingly, FXR activation impacts two well-known target genes of leptin, involved in cell proliferation, survival and motility as Cyclin D1, an important regulator of the cell cycle progression, and Survivin, a member of the inhibitor of apoptosis protein family (*Saxena N. K. et al., 2007; Jiang H. et al., 2008; Knight B. B. et al., 2011; Zheng Q. et al., 2012; Palianopoulou M. et al., 2011*). Moreover, the FXR ligand induces a decrease on leptin-mediated up-regulation of its own gene (*Ob*) expression, highlighting how this nuclear receptor is able to negatively interfere in the short autocrine loop maintained by leptin on *Ob* gene in breast cancer cells.

The above described effects were strictly dependent on FXR activation since they disappear in the presence of the dominant negative FXR plasmid. Mechanistically, we discovered that activated FXR counteracts leptin action on breast cancer cells through its ability to induce the expression of the suppressor of cytokine signaling 3 (SOCS3), a prototype molecule of the SOCS family. SOCS proteins are negative regulators of the JAK/STAT pathway and inhibit cytokine signaling by preventing JAK activity or by promoting protein degradation (Croker B. A. et al., 2008; Frantsve J. et al, 2001; Kamizono S. et al, 2001; Nicholson S. E. et al., 2000). SOCS3 has been identified as an inducible suppressor of leptin signaling, and in breast cancer cells, its overexpression has been shown to decrease proliferation and anchorage-independent growth (Palianopoulou M. et al., 2011). Recently, SOCS3 was recognized as a direct FXR target gene. Indeed, it has been demonstrated, in hepatocytes, that FXR ligands upregulate SOCS3 expression by enhancing its promoter activity (Xu Z. et al., 2012). Besides, FXR<sup>-/-</sup> knockout mice exhibit reduced basal expression of SOCS3, whereas activation of FXR by GW4064 induces SOCS3 mRNA levels in wild-type but not in FXR<sup>-/-</sup> mice (Li G. et al., 2013). In line with these

observations, our study demonstrated a direct involvement of FXR in positively modulating SOCS3 expression as revealed by its increase at both mRNA and protein levels in cells treated with GW4064. Furthermore, data from knock-down experiments highlight the functional relevance of SOCS3 in mediating the inhibitory effects of activated FXR on leptin downstream signaling.

During breast carcinogenesis, the epithelial and stromal tissues coevolve not only through cell-cell contact but also by secretion of soluble effectors coming from surrounding stromal cells. Indeed, in breast cancer tissues, ductal carcinoma *in situ* (DCIS) exhibits, in the stroma compartment, changes in the gene expression in a greater extent respect to the invasive tumors (Ma X. J. et al., 2009). Since the basement membrane is largely intact in DCIS, this suggests that paracrine and endocrine effects are crucial in inducing these modifications. In this context, we previously demonstrated that CAFs, the principal cellular component of the stroma, express leptin receptor and secrete leptin, which sustains a short autocrine loop and is able to target tumor epithelial cells, enhancing breast cancer cell proliferation and invasiveness (Barone I. et al., 2012). In this study we show that

treatment with GW 4064 is able to reverse CAF-induced cancer cell growth and motility, suggesting that activated FXR, counteracting the leptin-dependent paracrine effects on breast cancer restrain the tumor-promoting activities exerted by CAFs. Given the crucial role of FXR in negatively regulating the leptin signaling and preventing cancer-promoting activities of CAFs on breast cancer cell lines, we extend our data investigating whether FXR agonist may influence CAF phenotype. Our results demonstrate that FXR is expressed in several CAFs derived from different patients and treatment with GW 4064 is able to induce the transcription of key FXR target genes, including SHP (Small Heterodimer Partner) and BSEP (Bile Salt Export Pump). Interestingly, we observed that activated FXR significantly reduce CAF motility, without influencing their proliferation capabilities. Accordingly, IPA analysis on FXR-modulated genes by RNA-sequencing highlights cellular movement as the most significantly represented biologic process. Furthermore, most of the genes significantly down-regulated after GW 4064 treatment are involved in motile processes, suggesting that activated FXR may be important in influencing malignant motile processes of CAFs. The acquisition of a remodeled cytoskeleton and a

motile phenotype are important steps in tissue invasion and metastasis establishment, and the Rho family proteins have been reported to mediate these processes. Biological significance of Rho proteins in regulating cell migration is now well established and at least 20 Rho family proteins have been identified in humans, the most widely characterized molecules for their effects on cell migration are Rho A-C, which regulate stress fibers and focal adhesion formation, and Rac 1-3 and Cdc42, which control membrane ruffling, and filopodium formation (*Schmitz A.A. et al., 2000*). Particularly, Rho proteins promote stress fibers and strong adhesion to ECM through focal adhesion formation (*O' Connor K. et al., 2011*). In agreement with these data, we observed a marked reduction in the activity of Rho family and Integrin proteins, with activation z-score of -1, -0,5 respectively, further highlight an important role for activated FXR in regulating CAF motility. It has been reported that an increase in actin stress fibers formation and contractility are common features of motile cells (*Ridley A.J. et al., 2003*). Indeed, our results reveal a reduction in stress fibers formation in GW 4064 -treated CAFs. It has been demonstrated that CAFs are related with cancer cells at all stages of cancer progression, due to their production of

growth factors, chemokines and extracellular matrix components which in turn facilitates the angiogenic recruitment of endothelial cells and pericytes. Therefore, we demonstrated how, through the activation of FXR is possible to reduce tumor promoting abilities of CAFs on breast cancer cells, due to the ability of GW 4064 to reduce CAF secreted soluble factors, including IGF-1 (Insulin Growth Factor-1), FGF-9 (Fibroblast Growth Factor 9), TGF- $\beta$ 3 (Transforming Growth Factor Beta 3) and others key mediators involved in the crosstalk tumor-stroma. Indeed, our data demonstrate how ER- $\alpha$  breast cancer cell lines, MCF-7 and T47D, cocultured with conditioned media derived from GW4064-treated CAFs, exhibit a significantly reduced anchorage-independent growth and migration. Recent findings revealed that GW 4064 could also exert anti-proliferative effect through an FXR activation independent manner (Singh N. et al., 2014). We validate the direct involvement of this nuclear receptor in modulating CAF behaviour, through the treatment of CAFs with a natural and selective FXR antagonist named Z-Guggulsterone, that significantly reverse the effects deriving from its ligand-mediated activation. Moreover, the physiological relevance of the inhibitory effects exerted by FXR ligand on breast tumor

cells is pointed out by our *in vivo* studies showing that GW4064 administration markedly reduced growth of both MCF-7 as well as MCF-7/CAF xenografts. These observations well correlated with previous reports from our research group demonstrating that FXR activation plays a crucial role in reducing breast cancer cell proliferation and in inhibiting testicular tumor growth *in vitro* and *in vivo* (Catalano S. *et al.*, 2012; Catalano S. *et al.*, 2010). Although the therapeutic strategies against breast cancer have been focused for long time on directly targeting the malignant cell itself, it is now well recognized that the specific control of the signaling coming from the surrounding stromal cells represents an even more compelling treatment option. Thus, our results, highlighting the ability of activated FXR to counteract leptin signaling and cancer promoting activities of CAFs responsible for mammary carcinogenesis, support the possibility that FXR ligands could represent a promising pharmacological tools to be exploited in the novel strategies for breast cancer treatment.

---

## REFERENCES

---

- Ahima, R. S. & Osei, S. Y. Leptin signaling. *Physiol Behav* 81, 223–241 (2004).
- Allred, D. C., Harvey, J. M., Berardo, M. & Clark, G. M. Prognostic and predictive factors in breast cancer by immunohistochemical analysis. *Mod Pathol* 11, 155–168 (1998).
- Andò S. & Catalano S. The multifactorial role of leptin in driving the breast cancer microenvironment. *Nat Rev Endocrinol* 8, 263–275 (2011).
- Andò S. et al. The Multifaceted Mechanism of Leptin Signaling within Tumor Microenvironment in Driving Breast Cancer Growth and Progression. *Front Oncol* 4, 340 (2014).
- Barone I. et al. Leptin mediates tumor-stromal interactions that promote the invasive growth of breast cancer cells. *Cancer Res* 72, 1416–1427 (2012).
- Calle E.E., Kaaks R. Overweight, obesity and cancer: Epidemiological evidence and and proposed mechanisms. *Nature Reviews Cancer* 4, 579-591 (2004).
- Catalano S. et al. Leptin induces, via ERK1/ERK2 signal, functional activation of estrogen receptor alpha in MCF-7 cells. *J Biol Chem* 279(19):19908-19915 (2004).
- Catalano S. et al. Evidence that leptin through STAT and CREB signaling enhances cyclin D1 expression and promotes human endometrial cancer proliferation. *J Cell Physiol* 218, 490–500 (2009).
- Catalano S. et al. Farnesoid X receptor, through the binding with steroidogenic factor 1-responsive element, inhibits

- aromatase expression in tumor Leydig cells. *J Biol Chem* 285, 5581–5593 (2010).
- Catalano S. et al. In vivo and in vitro evidence that PPAR gamma ligands are antagonists of leptin signaling in breast cancer. *Am J Pathol* 179, 1030–1040 (2011).
- Catalano S. et al. Inhibition of Leydig tumor growth by farnesoid X receptor activation: the in vitro and in vivo basis for a novel therapeutic strategy. *Int J Cancer* 132, 2237–2247 (2012).
- Catalano S. et al. Leptin enhances, via AP-1, expression of aromatase in the MCF-7 cell line. *J Biol Chem* 278, 28668–28676 (2003).
- Chen C. et al. Leptin-induced growth of human ZR-75-1 breast cancer cells is associated with up-regulation of cyclin D1 and c-Myc and down-regulation of tumor suppressor p53 and p21WAF1/CIP1. *Breast Cancer Res Treat* 98, 121–132 (2006).
- Cirillo D. et al. Leptin signaling in breast cancer: an overview. *J Cell Biochem* 105, 956–964 (2008).
- Cirri P. et al. Cancer associated fibroblasts: the dark side of the coin. *Am J Cancer Res.* 1(4): 482–497 (2011).
- Croker B. A., Kiu H. & Nicholson S. E. SOCS regulation of the JAK/STAT signalling pathway. *Semin Cell Dev Biol* 19, 414–422 (2008).
- De Gottardi A. et al. The bile acid nuclear receptor FXR and the bile acid binding protein IBABP are differently expressed in colon cancer. *Dig Dis Sci* 49, 982–989 (2004).

- Fiorio E. et al. Leptin/HER2 crosstalk in breast cancer: in vitro study and preliminary in vivo analysis. *BMC Cancer* 8, 305 (2008).
- Forman B. M. et al. Identification of a nuclear receptor that is activated by farnesol metabolites. *Cell* 81, 687–693 (1995).
- Frantsve J. et al. Socs-1 inhibits TEL-JAK2-mediated transformation of hematopoietic cells through inhibition of JAK2 kinase activity and induction of proteasome-mediated degradation. *Mol Cell Biol* 21, 3547–3557 (2001).
- Garofalo C. et al. Increased expression of leptin and the leptin receptor as a marker of breast cancer progression: possible role of obesity-related stimuli. *Clin Cancer Res* 12, 1447–1453 (2006).
- Giordano C., et al. Farnesoid X receptor inhibits tamoxifen-resistant MCF-7 breast cancer cell growth through downregulation of HER2 expression. *Oncogene* 30:4129-40 (2011).
- Giordano C, et al. Activated FXR inhibits leptin signaling and counteracts tumor-promoting activities of cancer-associated fibroblasts in breast malignancy. *Sci Rep-UK* 6:21782 (2016).
- Giordano C. et al. Leptin as a mediator of tumor-stromal interactions promotes breast cancer stem cell activity. *Oncotarget* 7(2):1262-1275 (2016).
- Giordano C. et al. Leptin increases HER2 protein levels through a STAT3-mediated up-regulation of Hsp90 in breast cancer cells. *Mol Oncol* 7(3):379-391 (2013).
- Guo S. et al. Notch, IL-1 and Leptin crosstalk outcome (NILCO) is critical for leptin-induced proliferation, migration and

- VEGF/VEGFR-2 expression in breast cancer. *PLoS One* 6(6):21467 (2011).
- Hanahan D. & Weinberg R. A. Hallmarks of cancer: the next generation. *Cell* 144, 646–674 (2011).
- Ishikawa M. et al. Enhanced expression of leptin and leptin receptor (OB-R) in human breast cancer. *Clin Cancer Res* 10(13):4325-4331 (2004).
- Jarde T. et al. Leptin and leptin receptor involvement in cancer development: A study on human primary breast carcinoma. *Oncol Rep* 19(4):905-911 (2006).
- Jemal A. et al. Cancer statistics. *CA Cancer J. Clin.*, 60 pp. 277–300 (2010).
- Jiang, H. et al. Upregulation of survivin by leptin/STAT3 signaling in MCF-7 cells. *Biochem Biophys Res Commun* 368, 1–5 (2008).
- Journe F. et al. Farnesol, a mevalonate pathway intermediate, stimulates MCF-7 breast cancer cell growth through farnesoid-Xreceptor- mediated estrogen receptor activation. *Breast Cancer Res Treat* 107, 49–61 (2008).
- Kalluri R. et al. Fibroblasts in cancer. *Nature Reviews Cancer* 6, 392-401 (2006).
- Kalluri R. et al. The biology and function of fibroblasts in cancer. *Nature Reviews Cancer* 16, 582–598 (2016).
- Kamizono S. et al. The SOCS box of SOCS-1 accelerates ubiquitin-dependent proteolysis of TEL-JAK2. *J Biol Chem* 276, 12530–12538 (2001).

- Knight B. B. et al. Survivin upregulation, dependent on leptin-EGFR-Notch1 axis, is essential for leptin-induced migration of breast carcinoma cells. *Endocr Relat Cancer* 18, 413–428 (2011).
- Kocarek T. A. et al. Use of dominant negative nuclear receptors to study xenobiotic-inducible gene expression in primary cultured hepatocytes. *J Pharmacol Toxicol Methods* 47, 177–187 (2002).
- Korkaya H. et al. Breast cancer stem cells, cytokine networks, and the tumor microenvironment. *The Journal of Clinical Investigation*.121(10):3804-3809 (2011).
- Koutsounas I. et al. Farnesoid X Receptor (FXR) from normal to malignant state. *Histol Histopathol* 27, 835–853 (2012).
- Li G. et al. Mechanisms of STAT3 activation in the liver of FXR knockout mice. *Am J Physiol Gastrointest Liver Physiol* 305, G829–837 (2013).
- Luo H. et al. Cancer-associated fibroblasts: a multifaceted driver of breast cancer progression. *Cancer Lett* 361, 155–163 (2015).
- Ma X. J. et al. Gene expression profiling of the tumor microenvironment during breast cancer progression. *Breast Cancer Res* 11, R7 (2009).
- Makishima M. et al. Identification of a nuclear receptor for bile acids. *Science* 284, 1362–1365 (1999).
- Mao Y. et al. Stromal cells in tumor microenvironment and breast cancer. *Cancer Metastasis Rev* 32, 303–315 (2013).

- Maran R. R. et al. Farnesoid X receptor deficiency in mice leads to increased intestinal epithelial cell proliferation and tumor development. *J Pharmacol Exp Ther* 328, 469–477 (2009).
- Miyazaki-Anzai S. et al. Dual activation of the bile acid nuclear receptor FXR and G-protein-coupled receptor TGR5 protects mice against atherosclerosis. *PLoS One* 9, e108270 (2014).
- Miyoshi, Y. et al. High expression of leptin receptor mRNA in breast cancer tissue predicts poor prognosis for patients with high, but not low, serum leptin levels. *Int J Cancer* 118, 1414–1419 (2006).
- Modica S. et al. Deciphering the nuclear bile acid receptor FXR paradigm. *Nucl Recept Signal* 8, 005 (2010).
- Modica S. et al. Nuclear bile acid receptor FXR protects against intestinal tumorigenesis. *Cancer Res* 68, 9589–9594 (2008).
- Nicholson S. E. et al. Suppressor of cytokine signaling-3 preferentially binds to the SHP-2-binding site on the shared cytokine receptor subunit gp130. *Proc Natl Acad Sci U S A* 97, 6493–6498 (2000).
- O'Connor K. et al. Dynamic functions of RhoA in tumor cell migration and invasion. *Small GTPases*. 4(3):141-147 (2013).
- Paget S. et al. Distribution of secondary growths in cancer of the breast. *Lancet* 571–573 (1889).
- Palianopoulou M. et al. The activation of leptin-mediated survivin is limited by the inducible suppressor SOCS-3 in MCF-7 cells. *Exp Biol Med* (Maywood) 236, 70–76 (2011).

- Park J. et al. Paracrine and endocrine effects of adipose tissue on cancer development and progression. *Endocr Rev* 32(4):550-570 (2011).
- Parks D. J. et al. Bile acids: natural ligands for an orphan nuclear receptor. *Science* 284, 1365–1368 (1999).
- Protani M. et al. Effect of obesity on survival of women with breast cancer: Systematic review and meta-analysis. *Breast Cancer Res Treat* 123(3):627-635 (2010).
- Quail D. F. & Joyce, J. A. Microenvironmental regulation of tumor progression and metastasis. *Nat Med* 19, 1423–1437 (2013).
- Rehnan A.G. et al. Incident cancer burden attributable to excess body mass index in 30 european countries. *Int J Cancer* 126(3):692-702 (2010).
- Rehnan A.G. et al. Body-mass index and incidence of cancer: A systematic review and meta-analysis of prospective observational studies. *Lancet* 371(9612):569-578 (2008).
- Revillion F. et al. Messenger rna expression of leptin and leptin receptors and their prognostic value in 322 human primary breast cancers. *Clin Cancer Res* 12(7 Pt 1):2088-2094 (2006).
- Ridley A.J. et al. Cell migration: integrating signals from front to back. *Science*; 302:1704–9 (2003).
- Saxena N.K. et al. Bidirectional crosstalk between leptin and insulin-like growth factor-i signaling promotes invasion and migration of breast cancer cells via transactivation of epidermal growth factor receptor. *Cancer Res* 68(23):9712-9722 (2008).

- Saxena N. K. & Sharma, D. Multifaceted leptin network: the molecular connection between obesity and breast cancer. *J Mammary Gland Biol Neoplasia* 18, 309–320 (2013).
- Saxena N. K. et al. Leptin-induced growth stimulation of breast cancer cells involves recruitment of histone acetyltransferases and mediator complex to CYCLIN D1 promoter via activation of Stat3. *J Biol Chem* 282, 13316–13325 (2007).
- Singh et al. Synthetic FXR Agonist GW 4064 is a modulator of multiple G protein-coupled receptors. *Mol endocrinol* 28 (5):669-673 (2014).
- Schmitz A.A. et al. Rho GTPases: signaling, migration, and invasion. *Exp Cell Res* 261:1–12 (2000).
- Soma D. et al. Leptin augments proliferation of breast cancer cells via transactivation of HER2. *J Surg Res* 149, 9–14 (2008).
- Swales K. E. et al. The farnesoid X receptor is expressed in breast cancer and regulates apoptosis and aromatase expression. *Cancer Res* 66, 10120–10126 (2006).
- Sweeney G. Leptin signalling. *Cell Signal* 14, 655–663 (2002).
- Taubes G. et al. Cancer research. Unraveling the obesity-cancer connection. *Science* 335(6064):28, 30-22 (2012).
- Vavassori P. et al. The bile acid receptor FXR is a modulator of intestinal innate immunity. *J Immunol* 183, 6251–6261 (2009).
- Vona-Davis L. & Rose D. P. Adipokines as endocrine, paracrine, and autocrine factors in breast cancer risk and progression. *Endocr Relat Cancer* 14, 189–206 (2007).

- Xu Z. et al. FXR ligands protect against hepatocellular inflammation via SOCS3 induction. *Cell Signal* 24, 1658–1664 (2012).
- Yang F. et al. Spontaneous development of liver tumors in the absence of the bile acid receptor farnesoid X receptor. *Cancer Res* 67, 863–867 (2007).
- Zheng Q. et al. Leptin regulates cyclin D1 in luminal epithelial cells of mouse MMTV-Wnt-1 mammary tumors. *J Cancer Res Clin Oncol* 138, 1607–1612 (2012).